Modeling, Identification and Control, Vol. 43, No. 2, 2022, pp. 55–77, ISSN 1890–1328

Collision avoidance for ASVs through trajectory planning: MPC with COLREGs-compliant nonlinear constraints

Emil H. Thyri [1] Morten Breivik [1]

[1] *Centre for Autonomous Marine Operations and Systems (AMOS), Department of Engineering Cybernetics, Norwegian University of Science and Technology (NTNU), Trondheim, Norway.*
E-mail: emil.h.thyri@ntnu.no, morten.breivik@ieee.org

Abstract

This article presents a trajectory planning method for autonomous surface vessels that is compliant with Rule 8 and rules 13-17 from the Convention on the International Regulations for Preventing Collisions at Sea (COLREGs). The method is suitable for operation in restricted waters, where it both handles collision avoidance with static obstacles, and also considers the available room to maneuver when determining the appropriate safe distance to other vessels. The trajectory planner is formulated as a finite-horizon nonlinear model predictive controller, minimizing the deviation from a reference trajectory and the acceleration. Collision avoidance with static obstacles is included through the use of convex free sets. Collision avoidance with other traffic is done by assigning so-called target ship domains to each vessel, and formulating constraints for that domain. COLREGs rules 13-15 and 17 are included by first classifying each vessel-to-vessel encounter to find which rule applies, and subsequently assigning an encounter-specific domain to the opposing vessel. The domain is designed so that if the trajectory does not violate the domain, compliance with COLREGs rules 13-15 and partial compliance with Rule 17 is ensured. Furthermore, compliance with COLREGs Rule 8 and Rule 16 is included through a novel method for calculating the objective function cost-gains. By constructing windows of reduced tracking error and acceleration cost, the start time, duration and magnitude of a maneuver can be controlled, and hence readily apparent maneuvers made in ample time can be facilitated. The method's effectiveness and its completeness in terms of COLREGs compliance is demonstrated through an extensive set of simulations of vessel-to-vessel encounters in open waters. Furthermore, the robustness of the method is demonstrated through a set of complex simulations in confined areas with several maneuvering vessels. In all simulations, the method demonstrates compliance with COLREGs Rule 8 and rules 13-17.

Keywords: Autonomous surface vessels, trajectory planning, trajectory optimization, collision avoidance, marine navigation, marine transportation, marine vehicles.

1 Introduction

Utilizing autonomy or high levels of automation to increase efficiency and reduce cost of current operations is a vision for several actors in maritime applications such as autonomous container vessels for short sea and inland shipping, see Wärtsilä (2021), DB Schenker (2022), The Maritime Executive (2022). Others see autonomy as an enabler to new markets and operations like Zeabuz (2022) and RoBoat (2021), who are proposing small autonomous passenger ferries as an urban mobility changemaker. Another motivator for devel-

doi:10.4173/mic.2022.2.2

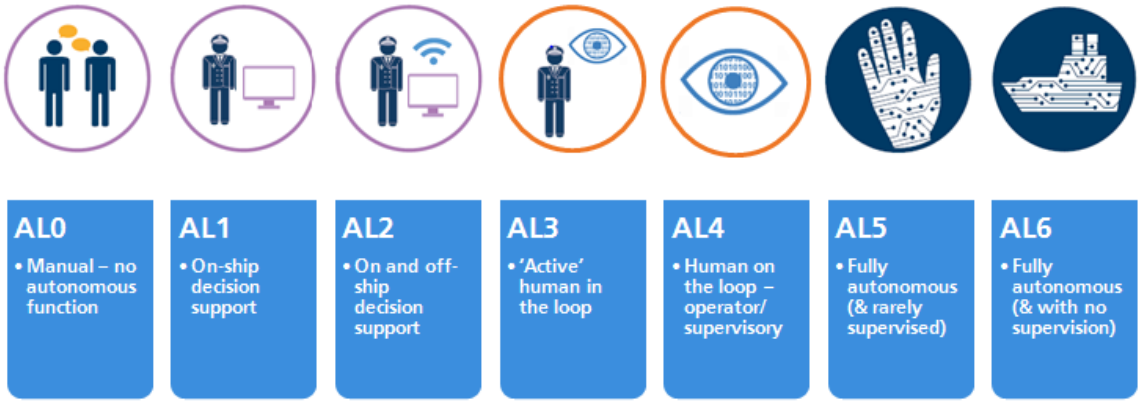

Figure 1: Levels of autonomy for maritime vessels. Courtesy of Lloyd's Register.

oping green autonomous vessels is reducing the strain on current land-based infrastructure by moving transportation to the underutilized waterways, and at the same time reduce the carbon footprint of operations by applying zero-emission vessels (Reddy et al., 2019; Čorić and Nikšić, 2022).

Introducing autonomy in maritime domains with other vessels or third parties is however not an overnight process. Like the automotive and aviation sector, maritime traffic is also subject to a set of rules and regulations, which any vessel upon the high seas, autonomous or not, must abide by. What makes this particularly challenging is that the Convention on the International Regulations for Preventing Collisions at Sea (COLREGs), which are "the rules of the road" on water, are developed over several centuries by sailors for sailors, and have several paragraphs that are left intentionally vague, and relies on the competence and experience of the navigator to evaluate the situation and make the correct choice of action. Furthermore, there are regulatory aspects that are not yet adapted to account for autonomous technology. In particular when the responsibility for comprehension and decision making is moved from human to machine, specific challenges related to this is further discussed by Ringbom (2019).

The development, deployment and operation of autonomous maritime vessels must therefore happen incrementally, and in parallel with the development of rules and regulations, so that assurance and thrust in the system can be build by all stakeholders. This can to a large extent be done through simulators, but must ultimately come through extensive operation. To aid this discussion between the technology and regulatory development, a taxonomy for maritime autonomy has been formulated by Lloyd's Register (2016), where seven levels of autonomy are defined, describing the distribution of jurisdiction and responsibility between the operator and the autonomy. The autonomy-levels are illustrated in Fig. 1, where they range from fully manual operation, through decision support and increasing autonomous control, where the operator take a supervisor role, and eventually is removed from and active role in the control of the vessel.

Replicating the capacity of a skilled operator or crew in an autonomous maneuvering system has proven hard to solve by one algorithm alone. This has led to the distribution of the planning, maneuvering and collision avoidance (COLAV) objectives in what is often referred to as a hybrid COLAV system (Loe, 2008). An example of a three-layer hybrid COLAV system is shown in Fig. 2. In such as a system, the high level planner considers long term strategic planning with objectives such as transit time, energy optimization and risk mitigation. The mid-level planner considers both dynamic and static obstacles, by making local adjustments to the global path or trajectory. In the case of supervised autonomy, it would fall on the mid-level COLAV method to produce a trajectory that assures the supervisor of the soundness of the autonomous maneuvering. The trajectory from the mid-level COLAV should therefore consider all the relevant rules from the COLREGs in the planning. The low-level COLAV also considers static and dynamic obstacles. It is responsible for the baseline safety of the maneuvering, and handles immediate and unforeseen situations. The system should consider COLREGs to the extent it is possible, and bring the vessel to a minimum risk condition if needed.

The main contribution of this paper is a deliberate COLAV method for autonomous surface vessels (ASVs) that handles both static and dynamic obstacles, and is compliant with COLREGs rules 8 and 13-17, regarding maneuvering in proximity to other vessels, and actions to avoid collision. The proposed method comprises a trajectory planner that is suitable for the mid-

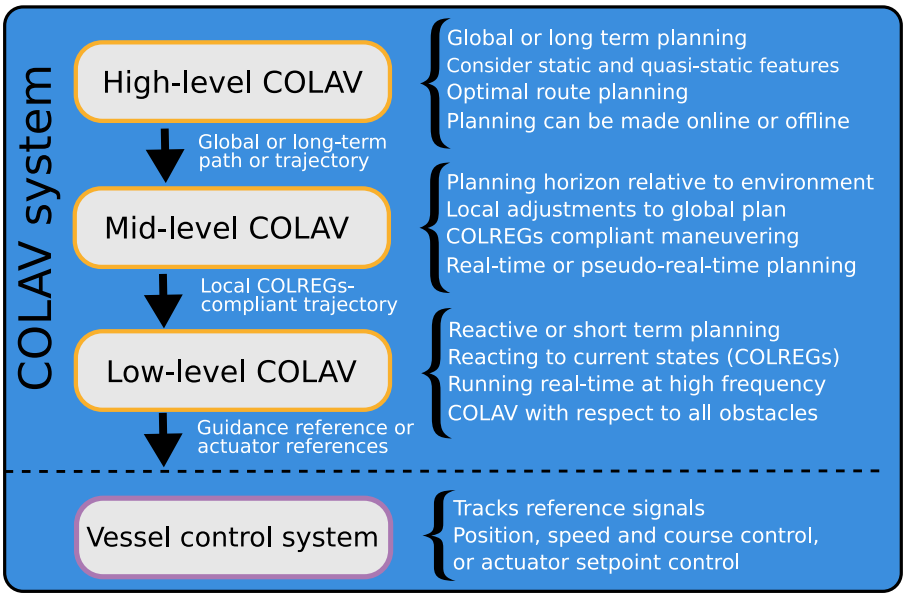

Figure 2: Three-layer hybrid COLAV structure, where the responsibility of path planning, trajectory planning, and reactive maneuvering is distributed over three separate methods. The figure is inspired by Eriksen and Breivik (2017).

level in a hybrid COLAV system like the one in Fig. 2, and has capacity suitable for autonomy-levels 3-6. The trajectory is calculated by formulating and solving an optimal control problem (OCP), where COLAV is enforced through inequality constraints. This work features two main novelties: (i) the constraints we formulate to enforce COLREGs rules 13-15 and 17, which are encounter-specific nonlinear constraints spanning both the position and velocity space, and (ii) the method for considering the more vague parts of the protocol, specifically Rule 8 and Rule 16, where we use dynamic cost-gain profiles with windows of reduced cost in the OCP objective function to control the timing and magnitude of a maneuver.

The remainder of this paper is structured as follows: Section 2 provides a review of relevant previous work. Section 3 presents theory on COLREGs, the target ship (TS) domain, and optimal control. In Section 4, we formulate the OCP, and present the features that ensure COLAV and COLREGs compliance. Section 5 presents simulation results, and Section 6 concludes the paper.

2 Previous work

In this section, a review of relevant previous work on collision avoidance for ASVs is presented. The review is not exhaustive, and for a more comprehensive overview, the reader is advised to consult Vagale et al. (2021b) and Öztürk et al. (2022), for a general review of planning, maneuvering and collision avoidance methods for ASVs, and Vagale et al. (2021a) for a comparative study.

One way to categorize algorithms for autonomous maneuvering and collision avoidance for ASVs is as reactive or deliberate algorithms. The reactive algorithms calculate an immediate action based on the current state of events, while the deliberate algorithms comprises capacity for planning for some horizon into the future, based on predictions of future states of events.

Some reactive algorithms applied to maritime surface vessels are the Velocity Obstacle (VO) algorithm in (Kuwata et al., 2014; Thyri and Breivik, 2022b), and the control barrier function (CBF)-based methods proposed by Thyri et al. (2020a) and Thyri and Breivik (2022a). These methods show some degree of COLREGs compliance, where they consider the maneuvering-specific rules 13-15 and 17. However, the reactive nature of the methods makes it challenging to consider the more general parts of the regulations such as rules 8 and 16 regarding making early and substantial maneuvers if circumstances of the case admit. Considering these regulations requires an understanding of the future states of the environment to enable a situation with considerable risk of collision to be resolved at an early stage, and hence avoid close quarters all together.

An approach to improving compliance with these rules is to apply trajectory-planning methods with a planning horizon extending a suitable time into the fu-

ture, as this enables improved deliberation when determining the optimal maneuver. A useful categorization of trajectory planning algorithms can be made w.r.t. its continuity. Discrete algorithms explore discrete parts of the configuration-space to find a trajectory connecting the start and goal position. Depending on the discretization method, the resulting trajectory has varying degrees of smoothness, and often require post-processing to ensure dynamic feasibility. In (Thyri et al., 2020b), a discrete trajectory planning method is proposed for an ASV canal crossing operation. The domain of dynamic obstacles are represented in a path-time space, and a visibility-graph is built and traversed to find a collision free trajectory connecting the start and goal. The method is demonstrated through a 3 hour continuous autonomous dock-to-dock operation in a canal in Trondheim[1]. The method proves effective for very short transit, such as canal crossing, but, lacks the maneuvering capacity for COLREGs-compliant maneuvering in a more general operational domain due to the path-velocity decomposition approach.

Alternatively, continuous methods, such as model predictive control (MPC), work in the continuous configuration-space by means of a dynamic vessel model. Such methods are popular in a wide range of applications, as they feature effective and versatile mechanisms for both formulating objectives for, and constraining, the system states in the control horizon. This makes them ideal for trajectory planning and collision avoidance, since primary objectives such as collision avoidance can be enforced through constraints, and secondary objectives such as path following, energy consumption, comfort or protocol adherence can be incentivized through the objective function.

In (Eriksen and Breivik, 2017; Xue et al., 2021; Abdelaal et al., 2018), nonlinear model predictive control is applied for ASV trajectory planning. The planners consider collision avoidance w.r.t. both static and dynamic obstacles by modeling them as circular domains and formulating constraints for the ASV position w.r.t. the circle boundaries. Furthermore, Eriksen and Breivik (2017) propose a cost function that favours readily apparent course change maneuvers in accordance with COLREGs Rule 8. However, COLREGs Part B regarding obligations of give-way and stand-on vessels is not considered. In (Xue et al., 2021) and (Abdelaal et al., 2018), COLREGs are considered through an increased cost on port maneuvers, and thereby favouring maneuvering to starboard. A similar approach is made in Abdelaal and Hahn (2016), where a soft constraint on the rate of change of yaw moment is applied to favour starboard maneuvers. All three methods demonstrate collision avoidance in encounters with a single TS in open waters. The robustness of the methods COLREGs compliance is however uncertain, since a bias towards starboard maneuvers provides little robustness to the principles of the protocol. Furthermore, without proper care, these mechanisms can also affect the maneuvering performance of the algorithms, by enforcing different response in port and starboard turns in situations without any dynamic obstacles. Additionally, the methods of modelling static obstacles as circular domains is feasible in areas with sparse island-like static features, however, it does not scale well to confined space with more complex obstacle geometry. This is considered by Martinsen et al. (2020), where an approach to docking for ASVs in urban areas is proposed. In the work, a convex set free of static obstacles is constructed around the ASV, allowing an arbitrary complex static obstacle environment to be represented by a small set of linear constraints.

A limiting factor to the COLREGs compliance of these methods is the TS domain they apply, which is the mechanism that ensures a safe distance between the vessels. Such domains have been applied by mariners for decades, either in collision risk warning systems, or as a tool for manually determining risk of collision. A critical review of such methods is given by Szlapczynski and Szlapczynska (2017), where they also propose a new ship domain for risk assessment. The use-case of these domains in risk assessment is however not the same as for autonomous maneuvering and collision avoidance algorithms. In the first case, the domains are used to determine the risk of collision, and if sufficient risk is deemed to exist, a navigator determines the appropriate action. For the second case, the TS domain is a mechanism that influences the nature of the manuever, since the trajectory is planned to not violate the domain. Therefore, TS domains for trajectory planning algorithms, should be designed to not only cover the state-space where risk of collision is high, but also the state-space that is in violation of the COLREGs.

In (Eriksen et al., 2019), a TS domain with COLREGs considerations is proposed for trajectory planning for a high-speed ASV in open waters. The domain is constructed from quarter ellipses with increased extension to the fore and starboard of the TS. The domain is enforced as a soft constraint, where the objective function carries a term of penalty as a function of the duration of the trajectory's violation of the domain. The shape of the domain incentivizes passing port to port in head-on encounters and behind in give-way crossing encounters. A disadvantage of using soft constraints for high priority objectives such as

[1] Video from the demonstration at:
https://www.youtube.com/watch?v=7i1Ykmdtic0&list=PLc2vvxBHfBcoHvfcIRsFROmJzXhbJCvb5&index=4&ab_channel=NTNUCybernetics

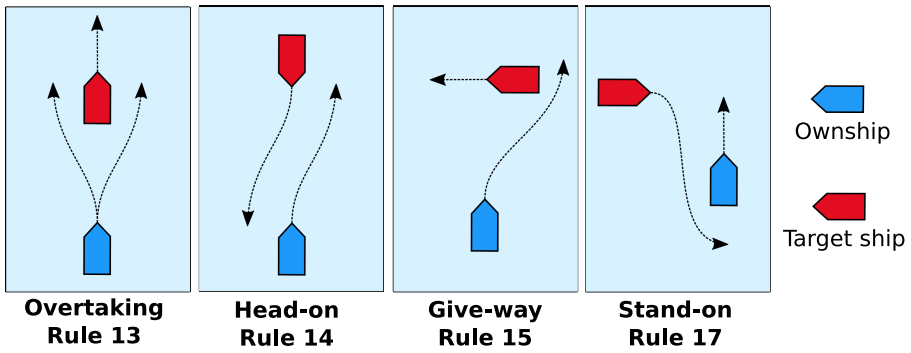

Figure 3: Illustration of COLREGs rules 13-15 and Rule 17, as seen from the OS in blue.

collision avoidance or COLREGs compliant maneuvering, is that they are often in conflict with other mission objectives such as path-following. Without a clear distinction between the mechanisms for enforcing the conflicting objectives, the trajectory planner is prone to plan a trajectory that is in conflict with the COLREGs or safety objective, but has an increased performance w.r.t. less critical objectives.

In (Thyri and Breivik, 2022a), an approach that mitigates this is presented. The authors propose a novel TS domain that is enforced through CBFs for a fully actuated ASV. The TS domain is designed explicitly for COLREGs compliance, and by formulating the CBFs w.r.t. both the distance to and velocity towards the domain, it is extended to also occupy regions in the combined position and velocity configuration-space. Through simulations, the authors demonstrate how the extended domain effectively covers COLREGs critical regions in the velocity-space without excessive extension in the position configuration-space, making it suitable for confined-space operation. Furthermore, through extensive simulations and full-scale experiments, the domain shows compliance with the encounter-type specific rules 13-15 and 17.

In this work, we apply the domain from (Thyri and Breivik, 2022a), by formulating hard constraints w.r.t. the distance to the domain boundary and the relative velocity towards the domain boundary, in order to ensure collision safety and to compliance with the encounter-type specific regulations. Furthermore, we expand the COLREGs compliance by predicting future risk of collision and considering rules 8 and 16 through maneuvering incentives in the objective function.

3 Background Theory

In this section, we introduce some background theory on the relevant rules from the COLREGs, and a method for classifying a vessel-to-vessel encounter w.r.t. COLREGs. Furthermore, the TS domain that we apply is described, and relevant theory on optimal control is provided.

3.1 COLREGs - The rules of the road

The COLREGs is the result of a convention developed over several centuries to prevent collision between two or more vessels at sea. It applies to all vessels upon the high seas and all waters connected to the high seas and navigable by seagoing vessels (Cockcroft and Lameijer, 2012).

The convention has four main parts: Part A - General, Part B - Steering and Sailing, Part C - Lights and Shapes and Part D - Sound and Light signals. In the work presented here, we consider maneuvering in the presence of other vessels in good visibility, and hence it is the rules in parts A and B, regarding vessels in sight of one another, that are most relevant. Here follows a short description of the rules we consider. Figure 3 illustrates vessel-to-vessel encounters where a subset of the rules applies to the ownship (OS).

- **Rule 8** *Any action to avoid collision shall, if circumstances of the case admit, be positive, made in ample time, and with due regard to good seamanship.*
- **Rule 13** *Any vessel overtaking another vessel shall keep out of the way of the vessel being overtaken. A vessel approaching another vessel from a direction of more than* 22.5 deg *abaft her beam is an overtaking vessel. Any subsequent alternation of bearing between the two vessels shall not relieve the overtaking vessel of the duty of keeping clear of the overtaken vessel until she is finally past and clear.*
- **Rule 14** *When two power-driven vessels are meeting on reciprocal or nearly reciprocal courses so as to involve risk of collision each shall alter her*

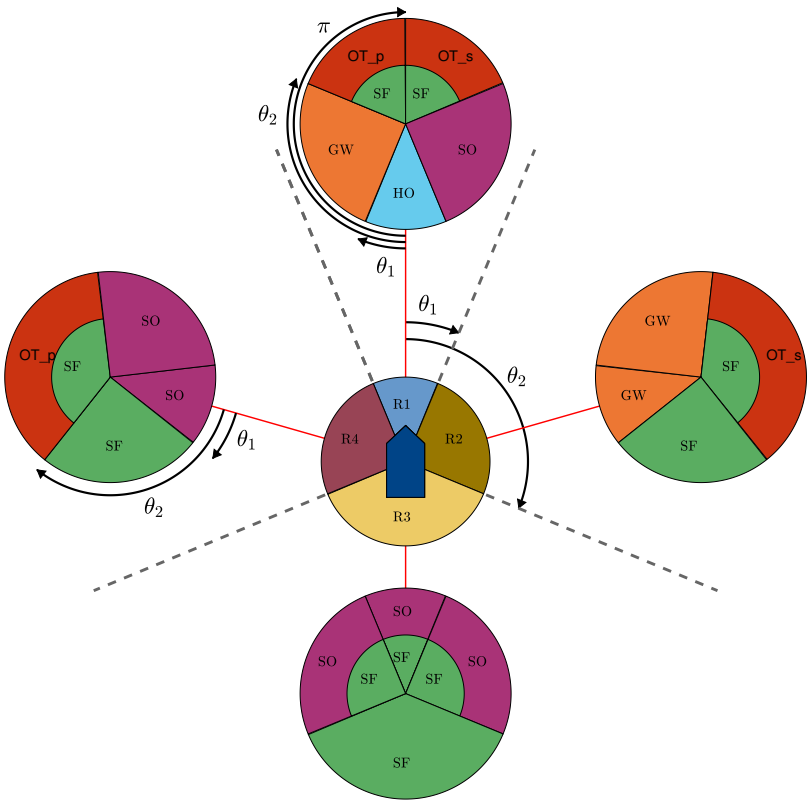

Figure 4: Graphic representation of the classification algorithm, where the position of the OS is at the center of the middle circle. In situation sectors with two encounter classifications, the outer one is chosen when the involved vessels have a closing range, while the inner one is chosen for increasing range.

course to starboard so that each shall pass on the port side of the other.

- **Rule 15** *When two power-driven vessels are crossing so as to involve risk of collision, the vessel which has the other on her own starboard side shall keep out of the way and shall, if the circumstances of the case admit, avoid crossing ahead of the other vessel.*

- **Rule 16** *Every vessel which is directed to keep out of the way of another vessel shall, so far as possible, take early and substantial action to keep well clear.*

- **Rule 17** *Where one of two vessels is to keep out of the way, the other shall keep her course and speed. The latter vessel may take action to prevent collision if it is apparent that the vessel required to keep out of the way is not taking appropriate action.*

Rules 13-15 and Rule 17 are specific to the encounter type, where only one of the rules applies to the OS. Therefore, to determine which rule applies, the encounter type must be determined. The criteria for classifying a vessel-to-vessel encounter are stated in the regulations, and classification is therefore a matter of calculating the required states and comparing them to the entry-criteria in the COLREGs. A method for this is proposed by Thyri and Breivik (2022a), where the proposed classification algorithm determines the encounter type to be one of the following, where the corresponding rule applies.

- Overtaking starboard side (OT_s): **Rule 13**
- Overtaking port side (OT_p): **Rule 13**
- Head-on (HO): **Rule 14**
- Give-way crossing (GW): **Rule 15**
- Stand-on crossing (SO): **Rule 17**
- Safe (SF): No rules apply

A graphical interpretation of the classification algorithm is shown in Fig. 4. In the figure, the OS is located at the center, with heading pointing up. The

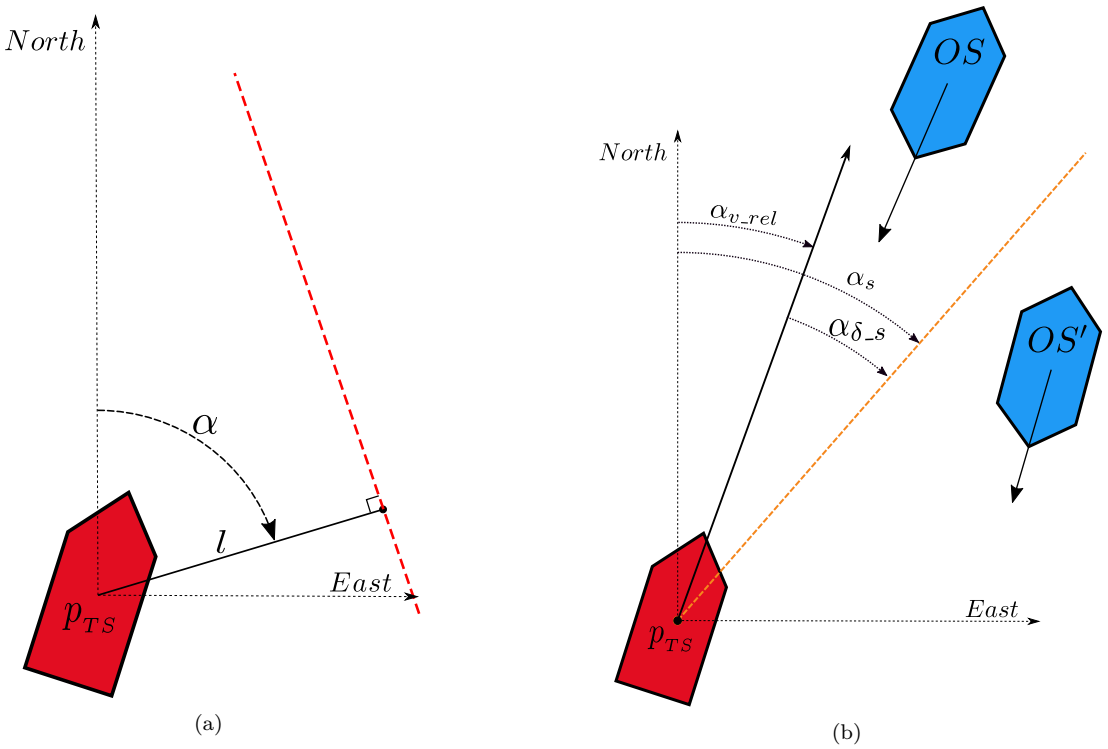

Figure 5: TS domain: a) TS domain defined by the angle α and the distance $l > 0$. b) Two instances of the OS on either side of the port-starboard split line.

area around the OS is split into four relative bearing sectors, where the relative bearing of the TS from the OS,

$$\varphi = \text{atan2}((E_{TS} - E), (N_{TS} - N)) - \chi, \tag{1}$$

along with the sector angles θ_1 and θ_2, is applied to determine the relative bearing sector to be one of R1, R2, R3 or R4. Here $[N, E]$ and $[N_{TS}, E_{TS}]$ are the north-east positions of the OS and TS in a local NED frame, and χ is the course of the OS. Subsequently, the encounter type is determined by the relative course of the TS to the OS

$$\chi_{rel} = \chi_{TS} - \chi, \tag{2}$$

where χ_{TS} is the course of the TS, along with a set of rotated sector angles $\theta_1^{'}$ and $\theta_2^{'}$, where $\theta_1^{'} = \theta_1 - \varphi_{TS}$ and $\theta_2^{'} = \theta_2 - \varphi_{TS}$, and

$$\varphi_{TS} = \text{atan2}((E - E_{TS}), (N - N_{TS})), \tag{3}$$

is the bearing of the OS from the TS. For further details on the classification method, see (Thyri and Breivik, 2022a).

3.2 Target ship domain

In this work, we apply the TS domain from (Thyri and Breivik, 2022a). The domain is designed so that if the OS maneuvers in such a way that it does not enter the TS domain, it also maneuvers in compliance with COLREGs rules 13-15 and 17. The proposed domain is specific to each TS, and is a function of the geometry and relative velocity of the encounter, the encounter type, and the available space to maneuver.

The TS domain is defined by a straight line dividing the north-east plane into two halves, where the TS is within one of the halves. An illustration of the domain is shown in Fig. 5(a) for a red TS. From the figure, one can see that in addition to the position of the TS at p_{TS}, the TS domain is defined by two variables: The shortest distance from the TS to the TS domain, denoted $l > 0$, and the angle of the normal vector to the domain boundary pointing away from the TS, denoted $\alpha \in (-\pi, \pi]$.

The orientation of the domain is a function of geometry and relative velocity of the encounter, in addition to encounter-type specific parameters. To determine the angle α, first the side of the OS that the TS should be when passing it is determined. This is determined by the bearing of the OS from the TS relative to a port-starboard split angle

$$\alpha_s = \alpha_{v\_rel} + \alpha_{\delta\_s}, \tag{4}$$

where α_{δ_s} is an encounter-type specific bias towards

maneuvering to the rules-compliant side, and α_{v_rel} is the angle of the relative velocity vector

$$\boldsymbol{v}_{rel} = \boldsymbol{v}_{TS} - \boldsymbol{v}, \tag{5}$$

with $\boldsymbol{v} = [\dot{N}, \dot{E}]^\mathsf{T}$ and $\boldsymbol{v}_{TS} = [\dot{N}_{TS}, \dot{E}_{TS}]^\mathsf{T}$ are the north-east velocities of the OS and TS, respectively. The angle α is defined as

$$\alpha := \begin{cases} \varphi_{TS} + \alpha_d, & \text{if } \varphi_{TS} > \alpha_s, \\ \varphi_{TS} - \alpha_d, & \text{else.} \end{cases} \tag{6}$$

where $\alpha_d \in (-\pi/2, \pi/2)$ is the deflection angle, which is an encounter-type specific parameter. This angle is used to facilitate passing the TS with a geometry that complies with the relevant rule.

The minimum distance from the TS to the domain line, and hence the minimum allowable distance between the OS and the TS, is

$$l = \begin{cases} r_{dyn} & \text{if } r_{free} \leq 0, \\ r_{dyn} + k_l r_{free} & \text{if } r_{free} \in (0, r_{free\_max}), \\ r_{dyn} + k_l r_{free\_max} & \text{if } r_{free} \geq r_{free\_max}. \end{cases} \tag{7}$$

where r_{free} is an estimate of the available free space to maneuver on the side of the TS that the OS should pass, while

$$r_{dyn} = \frac{1}{2}(l_{OS} + l_{TS}) + \delta_{dyn}, \tag{8}$$

is the minimum distance at which no collision will occur between the OS and TS independent of the encounter geometry. Here, l_{OS} and l_{TS} are the lengths of the OS and TS respectively, and $\delta_{dyn} > 0$ is an additional tolerance. Furthermore, r_{free} is a measure of the available space for the OS to maneuver between the TS and any static obstacles on the side of the TS that the OS will pass, and $k_l \in [0, 1]$ splits the free maneuverable space between the TS and a potential static obstacle. The parameter $r_{free\_max} > 0$ limits the contribution to l from the available space, and hence saturates the domain size in unrestricted waters. For further details on the TS domain, the reader is advised to see (Thyri and Breivik, 2022a).

3.3 Optimal control problem

In this work, we consider a system on the form

$$\dot{\boldsymbol{x}} = \boldsymbol{f}(\boldsymbol{x}(t), \boldsymbol{u}(t)), \;\; \boldsymbol{x}(0) = \boldsymbol{x}_0 \tag{9}$$

where $\boldsymbol{f} : \mathbb{R}^n \times \mathbb{R}^m \to \mathbb{R}^n$, is locally Lipschitz, $\boldsymbol{x} \in D \in \mathbb{R}^n$ contains the states of the system and $\boldsymbol{u} \in \boldsymbol{U} \in \mathbb{R}^m$ is the control input. This model applies to a variety of field robotics systems in air, on land and at sea.

A general OCP for such a system can be formulated as

$$\begin{aligned} \text{minimize} \quad & \theta(\boldsymbol{x}(t), \boldsymbol{u}(\boldsymbol{t})) \\ \text{subject to} \quad & \dot{\boldsymbol{x}}(t) = \boldsymbol{f}(\boldsymbol{x}(t), \boldsymbol{u}(t)) \\ & \boldsymbol{h}(\boldsymbol{x}(t), \boldsymbol{u}(t)) \geq \boldsymbol{0} \\ & \boldsymbol{x}(t_0) = \bar{\boldsymbol{x}}_{t_0} \end{aligned} \tag{10}$$

where $\theta : \mathbb{R}^n \times \mathbb{R}^m \to \mathbb{R}$ is the objective function, $\boldsymbol{h} : \mathbb{R}^n \times \mathbb{R}^m \to \mathbb{R}^{n_h}$ forms a set of n_h inequality constraints, and $\bar{\boldsymbol{x}}_{t_0} \in \mathbb{R}^n$ is the system state at $t = t_0$.

While such continuous OCPs in some cases can be solved analytically, this is generally not feasible. Instead, the problem is discretized and solved by nonlinear programming (NLP). In this paper, we apply a direct multiple shooting approach, where the system state and control input at each discretization step are explicitly defined as decision variables. The OCP with N_p discretized steps in the control horizon then becomes

$$\begin{aligned} \text{minimize} \quad & \theta(\boldsymbol{\omega}) \\ \text{subject to} \quad & \boldsymbol{g}(\boldsymbol{\omega}) = \boldsymbol{0} \\ & \boldsymbol{h}(\boldsymbol{\omega}) \geq \boldsymbol{0} \end{aligned} \tag{11}$$

where $\boldsymbol{\omega} = [\boldsymbol{x}_0^\mathsf{T}, \boldsymbol{u}_0^\mathsf{T}, ..., \boldsymbol{x}_{N_p-1}^\mathsf{T}, \boldsymbol{u}_{N_p-1}^\mathsf{T}, \boldsymbol{x}_{N_p}^\mathsf{T}]^\mathsf{T} \in \mathbb{R}^{(n+m)N_p+n}$ is a vector of decision variables, $\theta(\boldsymbol{\omega})$ is the objective function, $\boldsymbol{g}(\omega)$ is a set of equality constraints and $\boldsymbol{h}(\boldsymbol{\omega})$ is a set of inequality constraints.

When using multiple shooting, the vessel model (9) is enforced by formulating shooting constraints that are included in $\boldsymbol{g}(\omega)$. For this, an integrating function is applied to integrate the system states at timestep k subject to the control input at timestep k for the duration of the discretization step $h > 0$ to get the system states at timestep $k + 1$,

$$\boldsymbol{x}_{k+1} = \boldsymbol{F}(\boldsymbol{x}_k, \boldsymbol{u}_k). \tag{12}$$

One candidate for such an integrating function is the 4th order Runge Kutta method

$$\begin{aligned} k_1 &= \boldsymbol{f}(\boldsymbol{x}_k, \boldsymbol{u}_k) \\ k_2 &= \boldsymbol{f}(\boldsymbol{x}_k + \frac{h}{2} k_1, \boldsymbol{u_k}) \\ k_3 &= \boldsymbol{f}(\boldsymbol{x}_k + \frac{h}{2} k_2, \boldsymbol{u_k}) \\ k_4 &= \boldsymbol{f}(\boldsymbol{x}_k + h k_3, \boldsymbol{u_k}) \\ \boldsymbol{F}(\boldsymbol{x}_k, \boldsymbol{u}_k) &= \boldsymbol{x}_k + \frac{h}{6}\left(k_1 + 2k_2 + 2k_3 + k_4\right). \end{aligned} \tag{13}$$

The shooting constraints are defined as

$$\boldsymbol{g}(\boldsymbol{w}) = \begin{bmatrix} \bar{\boldsymbol{x}}_{t_0} - \boldsymbol{x}_0 \\ \boldsymbol{F}(\boldsymbol{x}_0, \boldsymbol{u}_0) - \boldsymbol{x}_1 \\ \boldsymbol{F}(\boldsymbol{x}_1, \boldsymbol{u}_1) - \boldsymbol{x}_2 \\ \vdots \\ \boldsymbol{F}(\boldsymbol{x}_{N_p-1}, \boldsymbol{u}_{N_p-1}) - \boldsymbol{x}_{N_p} \end{bmatrix}, \tag{14}$$

resulting in $n_g = n(N_p + 1)$ constraints.

4 OCP-based trajectory planner

In this section, the approach to COLREGs-compliant and collision-free maneuvering by trajectory planning is presented. The trajectory planning problem is formulated as an OCP, where collision avoidance is enforced through inequality constraints. Furthermore, COLREGs rules 13-15 and 17 are encoded in the constraints for the dynamic obstacles, and rules 8 and 16 are included through dynamic cost gains in the OCP objective function.

4.1 System model

The system model that we apply is a simple model on the form

$$\dot{\boldsymbol{x}} = \begin{bmatrix} \boldsymbol{v} \\ \boldsymbol{a} \end{bmatrix} \tag{15}$$

where $\boldsymbol{x} = [\boldsymbol{p}^\mathsf{T}, \boldsymbol{v}^\mathsf{T}]^\mathsf{T}$ is the system state vector and $\boldsymbol{a}$ is the control input. Here,

$$\boldsymbol{p} = \begin{bmatrix} N \\ E \end{bmatrix}, \tag{16}$$

is the north-east position of the system

$$\boldsymbol{v} = \begin{bmatrix} \dot{N} \\ \dot{E} \end{bmatrix}, \tag{17}$$

is the north-east velocity of the system, and

$$\boldsymbol{a} = \begin{bmatrix} \ddot{N} \\ \ddot{E} \end{bmatrix}, \tag{18}$$

is the north-east acceleration of the system. In choice of system model, the objectives of the OCP should be considered. High-fidelity vessel models allow for optimal control w.r.t. features such as energy efficiency, and by including actuator dynamics, non-holonomic properties of underactuated vessels can be considered. However, increased model complexity and nonlinearity comes at the cost of increased runtime, which can be decisive for the feasibility of applying OCPs in real-time applications. Therefore, care should be taken so that the fidelity of the model is sufficient for its purpose, without introducing unnecessary complexity. The trajectory planner we propose is intended as a mid-level COLAV method in a hybrid structure like the one shown in Fig. 2, where lower levels of the hybrid architecture considers higher fidelity vessel dynamics. Since the control objectives of the OCP that we propose are a function of the vessel position, velocity and acceleration, it is sufficient to apply a second-order linear system as in (15). Furthermore, by formulating constraints on the velocity states and the control input, feasibility of the optimal trajectory with respect to the actual vessel dynamics can still be ensured.

4.2 Problem definition and notation

The problem at hand is to plan a trajectory for the system in (15) that extends for some finite time horizon of duration

$$T_{horizon} = N_p h \tag{19}$$

from the current time, where $N_p > 0$ is the number of steps in the horizon, and $h > 0$ is the discretization interval. The inputs to the problem are:

1. A discretized reference trajectory $\boldsymbol{x}_{ref}$, which is used to calculate a desired trajectory for the OS extending throughout the planning horizon, on the form

   $$\boldsymbol{x}_d = [\boldsymbol{p}_{d,1}^\mathsf{T}, \boldsymbol{v}_{d,1}^\mathsf{T}, \boldsymbol{p}_{d,2}^\mathsf{T}, \boldsymbol{v}_{d,2}^\mathsf{T}, ..., \boldsymbol{p}_{d,N_p}^\mathsf{T}, \boldsymbol{v}_{d,N_p}^\mathsf{T}]^\mathsf{T} \tag{20}$$

   where

   $$\boldsymbol{p}_{d,k} = \begin{bmatrix} N_{d,k} \\ E_{d,k} \end{bmatrix}, \tag{21}$$

   is the desired position at timestep k and

   $$\boldsymbol{v}_{d,k} = \begin{bmatrix} \dot{N}_{d,k} \\ \dot{E}_{d,k} \end{bmatrix}, \tag{22}$$

   is the desired velocity at timestep k. In Section 4.6, we discuss how we calculate $\boldsymbol{x}_d$ from $\boldsymbol{x}_{ref}$.

2. A discretized trajectory prediction for every TS in line of sight from the OS, and the TS size. The predicted trajectory for TS i is on the form

   $$\boldsymbol{x}_{TS\_i} = [\boldsymbol{p}_0^{TS\_i}, \boldsymbol{v}_0^{TS\_i}, \boldsymbol{p}_1^{TS\_i}, \boldsymbol{v}_1^{TS\_i}, ..., \boldsymbol{p}_{N_p}^{TS\_i}, \boldsymbol{v}_{N_p}^{TS\_i}], \tag{23}$$

   where $\boldsymbol{p}_k^{TS\_i}$ and $\boldsymbol{v}_k^{TS\_i}$ are the predicted position and velocity of the TS at timestep k.

3. A map of static obstacles.

The objective is to calculate a trajectory that tracks the desired trajectory $\boldsymbol{x}_d$ with minimal tracking error,

while at the same time minimizes the control input. To achieve this, we proposed to use the objective function

$$\phi(\boldsymbol{p}, \boldsymbol{a}) = \sum_{k=0}^{N_p-1} \tilde{\boldsymbol{p}}_{k+1}^{\mathsf{T}} K_{k+1}^{p} \tilde{\boldsymbol{p}}_{k+1} + \boldsymbol{a}_k^{\mathsf{T}} K_k^{a} \boldsymbol{a}_k \tag{24}$$

where

$$\tilde{\boldsymbol{p}}_k = \boldsymbol{p}_k - \boldsymbol{p}_{d,k}, \tag{25}$$

is the relative error to the desired position at timestep k, and $K_k^p > 0$ and $K_k^a > 0$ are the cost-gains at timestep k for the position error and acceleration, respectively.

The output of the problem is a discretized trajectory on the form

$$\boldsymbol{x}^{opt} = [\boldsymbol{a}_0^{opt}, \boldsymbol{p}_1^{opt}, \boldsymbol{v}_1^{opt}, \tag{26}$$

$$\boldsymbol{a}_1^{opt}, \boldsymbol{p}_2^{opt}, \boldsymbol{v}_2^{opt}, ... \tag{27}$$

$$\boldsymbol{a}_{N_p-1}^{opt}, \boldsymbol{p}_{N_p}^{opt}, \boldsymbol{v}_{N_p}^{opt}] \tag{28}$$

that is optimal w.r.t. the cost function (24) while adhering to the constraints of $\boldsymbol{g}$ and $\boldsymbol{h}$, which will be defined shortly. The first term of $\phi(\boldsymbol{p}, \boldsymbol{a})$ in (24) motivates the optimal trajectory to track the desired trajectory by minimizing the tracking error at each timestep, while the second motivates a smooth trajectory by penalizing acceleration. For a dynamic trajectory, these two objectives are conflicting. The same is true for situations where another vessel is in conflict with the desired trajectory and an avoidance maneuver resulting in both tracking error and acceleration usage is required. However, by appropriately assigning the cost-gain profiles for the control horizon, a satisfactory compromise can be reached. The design of the cost-gain profiles is discussed in Section 4.8

4.3 Constraints for trajectory feasibility

To ensure feasibility of the trajectory, inequality constraints for the velocity state $\boldsymbol{v}_k \forall k \in [1, N_p]$ and control input $\boldsymbol{a}_k \forall k \in [0, N_p - 1]$ are formulated. The velocity constraints are formulated as

$$\boldsymbol{h}_v = \begin{bmatrix} U_{max}^2 - \boldsymbol{v}_1^{\mathsf{T}} \boldsymbol{v}_1 \\ U_{max}^2 - \boldsymbol{v}_2^{\mathsf{T}} \boldsymbol{v}_2 \\ \vdots \\ U_{max}^2 - \boldsymbol{v}_{N_p}^{\mathsf{T}} \boldsymbol{v}_{N_p} \end{bmatrix} \tag{29}$$

where $U_{max} > 0$ is the upper velocity limit for the trajectory. In the same way, the constraints on acceleration are formulated as

$$\boldsymbol{h}_a = \begin{bmatrix} a_{max}^2 - \boldsymbol{a}_0^{\mathsf{T}} \boldsymbol{a}_0 \\ a_{max}^2 - \boldsymbol{a}_1^{\mathsf{T}} \boldsymbol{a}_1 \\ \vdots \\ a_{max}^2 - \boldsymbol{a}_{N_p-1}^{\mathsf{T}} \boldsymbol{a}_{N_p-1} \end{bmatrix} \tag{30}$$

where $a_{max} > 0$ is the upper acceleration limit for the trajectory. To ensure dynamic feasibility of the trajectory, U_{max} and a_{max} should reflect the maneuvering capacity of the vessel.

4.4 Constraints for dynamic obstacles

The constraints for the dynamic obstacles are formulated with respect to the TS domain introduced in Section 3. The TS domain is designed with broad consideration to the COLREGs, so that as long as it is not violated, the trajectory will be collision-free with dynamic obstacles, and comply with COLREGs rules 13-15 and Rule 17.

The constraint is formulated with respect to the point

$$\boldsymbol{p}_B = \boldsymbol{p}_D + (\boldsymbol{p} - \boldsymbol{p}_D)^{\mathsf{T}} \boldsymbol{n}_{p_D} \boldsymbol{n}_{p_D}, \tag{31}$$

which is the point on the TS domain closest to the OS, where

$$\boldsymbol{p}_D = \boldsymbol{p}_{TS} + \boldsymbol{n}_D l \tag{32}$$

is the point on the TS domain closest to the TS,

$$\boldsymbol{n}_D = \begin{bmatrix} \cos(\alpha) \\ \sin(\alpha) \end{bmatrix} \tag{33}$$

is the normal vector to the domain boundary pointing out of the domain, and

$$\boldsymbol{n}_{p_D} = \begin{bmatrix} -\sin(\alpha) \\ \cos(\alpha) \end{bmatrix} \tag{34}$$

is the tangent vector to the domain boundary.

The constraint is then defined as the distance from the position of the OS at $\boldsymbol{p}$ to the domain

$$h_{TS}(\boldsymbol{p}, \boldsymbol{p}_{TS}) = \boldsymbol{n}_D^{\mathsf{T}}(\boldsymbol{p} - \boldsymbol{p}_B). \tag{35}$$

In addition to the constraint in (35), we propose to use an augmented constraint that not only considers the distance to the domain, but also the velocity at which the OS is approaching the domain. The augmented constraint is defined as

$$h_{TS}(\boldsymbol{p}, \boldsymbol{v}, \boldsymbol{p}_{TS}, \boldsymbol{v}_{TS}) = \boldsymbol{n}_D^{\mathsf{T}}(\boldsymbol{p} - \boldsymbol{p}_B) + c_{dyn} \boldsymbol{n}_D^{\mathsf{T}}(\boldsymbol{v} - \boldsymbol{v}_B) \tag{36}$$

where $\boldsymbol{v}_B$ is the velocity of the point $\boldsymbol{p}_B$, given by

$$\begin{aligned} \dot{\boldsymbol{p}}_B =& \dot{\boldsymbol{p}}_D + (\dot{\boldsymbol{p}} - \dot{\boldsymbol{p}}_D)^{\mathsf{T}} \boldsymbol{n}_{p_D} \boldsymbol{n}_{p_D} + (\boldsymbol{p} - \boldsymbol{p}_D)^{\mathsf{T}} \dot{\boldsymbol{n}}_{p_D} \boldsymbol{n}_{p_D} \\ &+ (\boldsymbol{p} - \boldsymbol{p}_D)^{\mathsf{T}} \boldsymbol{n}_{p_D} \dot{\boldsymbol{n}}_{p_D}. \end{aligned} \tag{37}$$

Here,

$$\dot{\boldsymbol{n}}_{p_D} = \frac{\partial \boldsymbol{n}_{p_D}}{\partial \alpha} \dot{\alpha}, \tag{38}$$

and

$$\dot{\boldsymbol{p}}_D = \dot{\boldsymbol{p}}_{TS} + \boldsymbol{n}_{p_D} l \dot{\alpha}, \tag{39}$$

is the velocity of the point $\boldsymbol{p}_D$. When formulating the constraints, we assume that the TS keeps a constant course and speed, and hence $\dot{\alpha} = \dot{\varphi}_{TS}$, with

$$\dot{\varphi}_{TS} = \left(\boldsymbol{R}_2(\tfrac{\pi}{2}) \frac{\bar{\boldsymbol{p}}}{\bar{\boldsymbol{p}}^\mathsf{T} \bar{\boldsymbol{p}}} \right)^\mathsf{T} \dot{\bar{\boldsymbol{p}}}, \tag{40}$$

where $\bar{\boldsymbol{p}} = \boldsymbol{p} - \boldsymbol{p}_{TS}$ and $\dot{\bar{\boldsymbol{p}}} = \boldsymbol{v} - \boldsymbol{v}_{TS}$ denote the relative position and velocity between the two vessels, respectively, and

$$\boldsymbol{R}_2(\phi) = \begin{bmatrix} \cos(\phi) & -\sin(\phi) \\ \sin(\phi) & \cos(\phi) \end{bmatrix}. \tag{41}$$

The parameter $c_{dyn} > 0$ in (36) mitigates between the distance to the domain, and the velocity at which the OS is allowed to approach the domain, and hence serves as an effective way of setting a lower threshold for when a maneuver to avoid collision should be initiated. This is in-line with Rule 8, regarding taking early action to avoid collision.

The constraints for TS_i for the control horizon is

$$\boldsymbol{h}_{TS\_i} = \begin{bmatrix} h_{TS}(\boldsymbol{p}_1, \boldsymbol{p}_1^{TS\_i}) \\ h_{TS}(\boldsymbol{p}_2, \boldsymbol{p}_2^{TS\_i}) \\ \vdots \\ h_{TS}(\boldsymbol{p}_{N_p}, \boldsymbol{p}_{N_p}^{TS\_i}) \end{bmatrix}, \tag{42}$$

and

$$\boldsymbol{h}_{\dot{T}S\_i} = \begin{bmatrix} h_{\dot{T}S}(\boldsymbol{p}_1, \boldsymbol{v}_1, \boldsymbol{p}_1^{TS\_i}, \boldsymbol{v}_1^{TS\_i}) \\ h_{\dot{T}S}(\boldsymbol{p}_2, \boldsymbol{v}_2, \boldsymbol{p}_2^{TS\_i}, \boldsymbol{v}_2^{TS\_i}) \\ \vdots \\ h_{\dot{T}S}(\boldsymbol{p}_{N_p}, \boldsymbol{v}_{N_p}, \boldsymbol{p}_{N_p}^{TS\_i}, \boldsymbol{v}_{N_p}^{TS\_i}) \end{bmatrix}, \tag{43}$$

resulting in $2N_p$ constraints for each TS, and the set of constraints for dynamic obstacles

$$\boldsymbol{h}_{TS} = \bigcup_{i}^{\mathcal{N}_{pri}} \left(\boldsymbol{h}_{TS\_i} \cup \boldsymbol{h}_{\dot{T}S\_i} \right), \tag{44}$$

where $\mathcal{N}_{pri}$ is the set of vessels to be considered. The construction of $\mathcal{N}_{pri}$ is discussed in Section 4.7.

4.5 Constraints for static obstacles

The approach propose for COLAV with static obstacles is to formulate a convex free set at the reference position of timesteps $k \in \mathcal{C}_{stat}$ where the set $\mathcal{C}_{stat} \subseteq \{1, 2, ..., N_p\}$. When designing the subset $\mathcal{C}_{stat}$, the dynamics of the vessel and discretization interval of the OCP should be considered to ensure safety, while at the same time avoiding excessive constraints and overhead related to lookups in map-data.

The convex free set for timestep k is constructed in the following way:

1. a set of N_{sect} non-overlapping equally sized sectors covering the complete circle around the reference position at $\boldsymbol{p}_{d,k}$ is defined
2. the closest point on any static obstacle within each sector is found by a search in the map data, where the points are denoted $\boldsymbol{p}_{stat\_i}, i \in [1, 2, ..., N_{sect}]$
3. a domain is assigned to each point $\boldsymbol{p}_{stat\_i}$ by constructing a normal vector $\boldsymbol{n}_{\boldsymbol{p}_{stat\_i}}$ for the point, and considering the domain boundary as the line passing through the point perpendicular to the normal vector. The normal vector for each point is found by the method in (Martinsen et al., 2020), where it is constructed to be normal to the boundary of, and pointing into, an ellipse centered in $\boldsymbol{p}_{d,k}$, with its major axis aligned with the desired course at timestep k, defined as

$$\chi_{d_k} := atan2(\dot{E}_{d,k}, \dot{N}_{d,k}), \tag{45}$$

and the relationship between the major and minor axis given by

$$\sigma = \begin{cases} \sigma_{min} \quad if\ d_{min} > d_{\sigma\_min} \\ \sigma_{max} - \rho(d_{min}) \quad if\ d_{min} \in [d_{\sigma\_max}, d_{\sigma\_min}] \\ \sigma_{max} \quad if\ d_{min} < d_{\sigma\_max} \end{cases}, \tag{46}$$

where

$$\rho(d_{min}) = (d_{min} - d_{\sigma\_max}) \frac{\sigma_{max} - \sigma_{min}}{d_{\sigma\_min} - d_{\sigma\_max}}, \tag{47}$$

and

$$d_{min} = \min_{i}^{N_{sect}} ||\boldsymbol{p}_{d,k} - \boldsymbol{p}_{stat\_i}||, \tag{48}$$

is the minimum distance from the reference position to any static obstacle, and $\sigma \in [\sigma_{min}, \sigma_{max}]$, and d_{σ_max} and d_{σ_min} are the distances at which σ has its minimum and maximum value respectively, where $d_{\sigma\_max} < d_{\sigma\_min}$.

Here, step 3 reduces the chances of restricting the optimal trajectory from traversing along the reference trajectory in very confined spaces by increasing the relationship between the major and minor axis in the ellipse, and hence stretching out the convex free set in the direction travel. However, when the distance to static obstacles is large, the relationship σ is decreased, and the convex free set takes a more circular form. This opens up the areas to the starboard and port of the reference trajectory for maneuvers. This is demonstrated by Fig. 6, where a convex free set is constructed at 70 s intervals along a reference trajectory. In the figure, the convex free set is more circular when the reference position has a larger margin to static obstacles, like the darker of the two green sets and the red set, while the

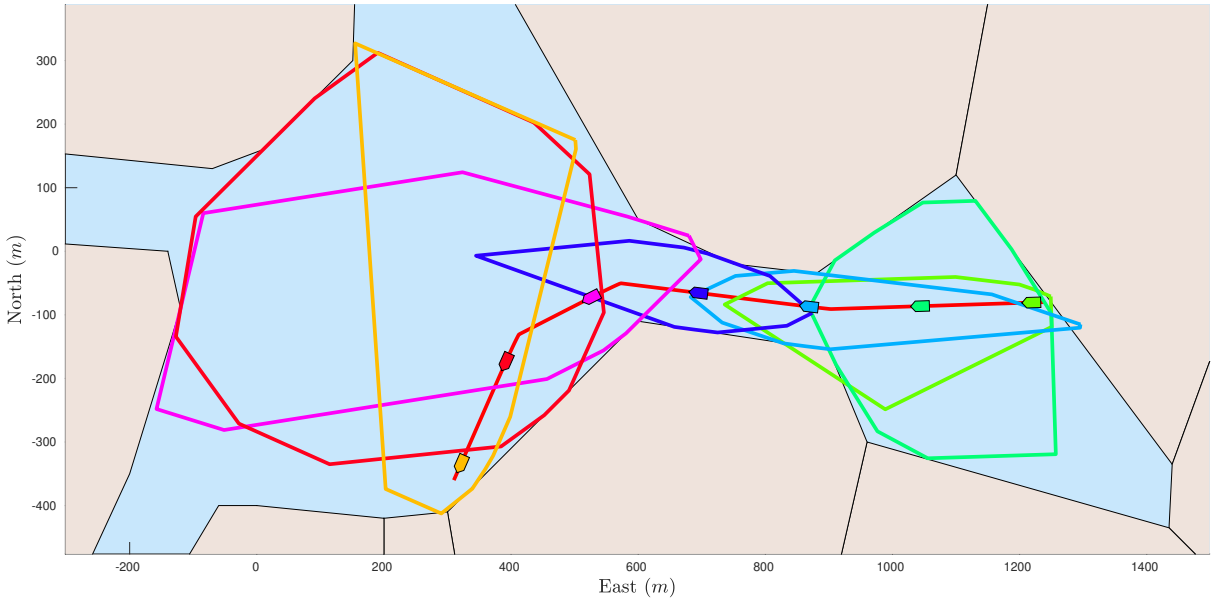

Figure 6: Convex free sets w.r.t. static obstacles with $N_{sect} = 12$. The figure shows sets for OS at intervals of 70 s along a reference trajectory in red. Color of set boundary correspond to color of vessel.

convex free set is more ellipse-shaped for the two blue sets, where the reference position is in a narrow area.

To constrain the trajectory to the convex free set, linear constraints are formulated as a function of the distance to the domain of each point $\boldsymbol{p}_{stat\_i}$

$$\boldsymbol{h}_{stat\_k} = \begin{bmatrix} \boldsymbol{n}^{\mathsf{T}}_{\boldsymbol{p}_{stat\_1}}(\boldsymbol{p}_k - \boldsymbol{p}_{stat\_1}) - \delta_{stat} \\ \boldsymbol{n}^{\mathsf{T}}_{\boldsymbol{p}_{stat\_2}}(\boldsymbol{p}_k - \boldsymbol{p}_{stat\_2}) - \delta_{stat} \\ \vdots \\ \boldsymbol{n}^{\mathsf{T}}_{\boldsymbol{p}_{stat\_N_{sect}}}(\boldsymbol{p}_k - \boldsymbol{p}_{stat\_N_{sect}}) - \delta_{stat} \end{bmatrix}, \tag{49}$$

where $\delta_{stat} > 0$ ensures a minimum distance to the obstacle. The complete set of constraints for static obstacles then becomes

$$\boldsymbol{h}_{stat} = \bigcup_{k}^{\mathcal{C}_{stat}} \boldsymbol{h}_{stat\_k}. \tag{50}$$

4.6 Reference trajectory

Since any dynamic obstacle can be passed on both sides, the proposed OCP is non-convex whenever a TS is considered. There is therefore a local minima to the OCP corresponding to a trajectory passing on either side of a TS, and the number of local minima increases exponentially with the number of TSs. Additionally, since avoidance maneuvers by definition will make the solution deviate from the reference trajectory, and hence increase the cost, the solver is prone to produce solutions that are oscillating between two or more local minima at successive iterations of the solver with minor changes in the problem input. Since, by design, each of the local minima are collision-free and partially COLREGs-compliant trajectories, it is not paramount to find the global minimum. However, fluctuations between several local minima at successive iterations can result in non-predictable OS behaviour, which is unfortunate and in conflict with the protocol requirements.

We propose to mitigate this by two means: First, a trajectory for an initial guess of the OCP, $\boldsymbol{x}_{initial\_guess}$, is calculated based on the time-shifted optimal solution from the previous iteration $\boldsymbol{x}_{opt\_prev}$. Padding at the end of the trajectory to extend it to match the control horizon is added by simulating a Nomoto model with LOS guidance with initial states that correspond to the end of the previous optimal trajectory. Assuming that any TS is maneuvering close to its predicted trajectory in the previous iteration, then $\boldsymbol{x}_{opt}$ will be close to $\boldsymbol{x}_{initial\_guess}$.

Secondly, the desired trajectory $\boldsymbol{x}_d$ for the OCP is calculated as a weighted average between the reference trajectory $\boldsymbol{x}_{ref}$ and the initial guess, as

$$\boldsymbol{x}_d = \kappa \boldsymbol{x}_{ref} + (1 - \kappa)\boldsymbol{x}_{initial\_guess}, \tag{51}$$

where $\kappa \in [0, 1)$ and $\boldsymbol{x}_{ref}$ is a discretized reference trajectory on the form of (20), where $\boldsymbol{x}_{ref}$ can be provided by an arbitrary higher level planner. Details on how we calculate $\boldsymbol{x}_{ref}$ is provided in Section 5. By appropriate choice of κ, the fluctuations between local minima at successive solutions of the OCP can be reduced by moving the current global optima closer to the previous optimal solution, and hence closer to the initial guess.

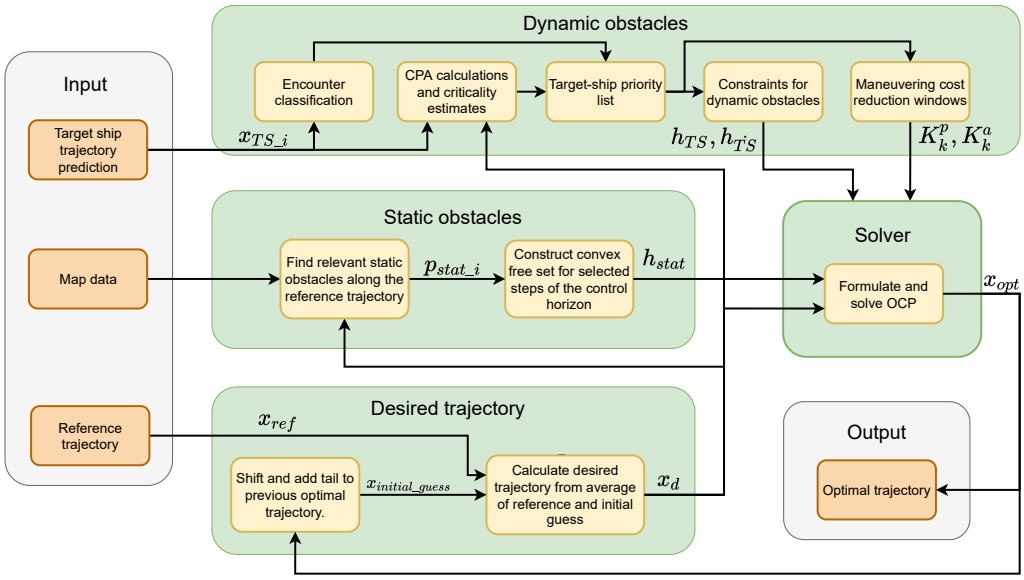

Figure 7: Overview of the pipeline for the proposed trajectory planning method.

The rationale behind this is that the COLAV objective has higher priority than the trajectory tracking objective, and that when $\boldsymbol{x}_{opt}$ deviates from $\boldsymbol{x}_{ref}$, it is a beneficial deviation w.r.t. safety and COLREGs compliance, and should be facilitated. If there are no constraints from dynamic or static obstacles in conflict with the input trajectory $\boldsymbol{x}_{ref}$, then both $\boldsymbol{x}_d$ and $\boldsymbol{x}_{initial\_guess}$ will converge to $\boldsymbol{x}_{ref}$, and hence the optimal solution $\boldsymbol{x}_{opt}$ will converge towards $\boldsymbol{x}_{ref}$, restricted only by the acceleration cost in (24).

4.7 Target ship priority

An operational domain can include several vessels, where the vessels might not interfere with the OS trajectory at all, and hence do not need to be assigned constraints in the OCP. Additionally, the OS might be in a stand-on encounter with vessels, and is therefore obliged, conditionally, to keeps its course and speed while the give-way vessel maneuvers, or until it is clear that the give-way vessel is not abiding its duty, and the encounter can not be resolved by maneuvering from the TS alone. Constraints should therefore not be assigned to vessels which the OS is in a stand-on encounter with, until the absence of a maneuver from the TS is apparent. To resolve this, we propose a list of prioritized vessels denoted $\mathcal{N}_{pri}$, where constraints are formulated only for vessels in $\mathcal{N}_{pri}$. The entry criteria are based on a critical distance at closest point of approach (DCPA), $d_{crit} > 0$, as well as the time until the OS enters and exits a circular region around the TS with radius d_{crit} , denoted t_{crit}^{enter} and t_{crit}^{exit}, respectively. For a TS with DCPA larger than d_{crit}, t_{crit}^{enter} and t_{crit}^{exit} are not defined, however by appropriate choice of d_{crit}, such a TS need not be included in $\mathcal{N}_{pri}$.

Target ships in encounters that are classified as either give-way, overtaking or head-on are included in the priority list if either

$$t_{crit}^{exit} < T_{horizon} - T_{after\_pass\_padding}, \tag{52}$$

or

$$t_{crit}^{enter} < T_{critical}. \tag{53}$$

The first criteria admits vessels to the list once the control horizon extends for a time $T_{after\_pass\_padding} > 0$ beyond the point where the previous optimal trajectory exits critical distance. This increasing the chances of $\boldsymbol{x}_{opt}$ to actually resolve the encounter with the relevant TS, and not for example reduce speed to avoid encountering the TS within the horizon. The second criteria ensures that the vessel is included in $\mathcal{N}_{pri}$ if t_{crit}^{enter} drops below a critical threshold $T_{critical} > 0$, even though t_{crit}^{exit} is not sufficiently in the control horizon. This is relevant for encounters where the relative velocity between the vessels is low e.g. in overtaking encounters. A TS in an encounter classified as stand-on is entered into the list if

$$t_{crit}^{enter} < T_{crit\_stand-on}. \tag{54}$$

Here, $T_{crit\_stand-on}$ serves as a threshold for when it is assumed that the TS is not abiding its give-way obligations, and the OS needs to take action to avoid collision.

4.8 Positive maneuvers in ample time

The features of the OCP described so far will ensure that $\boldsymbol{x}_{opt}$ is collision-free with static and dynamic obstacles while avoiding dynamic obstacles in a manner that is compliant with COLREGs rules 13-15 and 17. However Rule 8 and Rule 16 are yet to be addressed. Some regard was given to this by the introduction of the second constraint type for dynamic obstacles, where the relative velocity in the encounter is restricted by the range between the vessels. This does however only set a lower limit for the range to start a maneuver for a given relative velocity, but does not consider the magnitude of the maneuver, or whether it is initiated in ample time.

To improve compliance with rules 8 and 16, and facilitate readily apparent maneuvers made in ample time, we propose to design a cost profile for the gains of the cost function, namely K_k^p and K_k^a for $k \in [1, N_p]$. In particular, we design separate cost reduction windows (CRW) for the position and acceleration cost, where windows of reduced cost in the OCP horizon will facilitate a required maneuver to be made within that window. In particular, an acceleration cost reduction window (ACRW) will facilitate any maneuver to avoid or give-way to an oncoming vessel to happen within that window. Then it is only a matter of placing the ACRW so that it both starts and ends "in ample time" before t_{crit}^{enter} for that vessel to ensure that, if possible, the maneuver is completed within an appropriate time. Further, by assigning an appropriately short duration to this ACRW, the magnitude of the maneuver can also be manipulated. To allow the optimal trajectory to deviate from $\boldsymbol{x}_d$ from the start of the ACRW until the encounter is resolved, a position cost reduction window (PCRW) is assigned.

The design of the CRWs is made based on the estimated t_{crit}^{enter} and t_{crit}^{exit} for the vessels in $\mathcal{N}_{pri}$. The start time for the ACRW is

$$t_{ACRW}^{start} = \min_{\mathcal{N}_{pri}}(t_{crit}^{enter}) - T_{ample\_time}, \tag{55}$$

where $T_{ample\_time} > 0$ is an estimate for what is considered ample time for that specific encounter. The end time for the acceleration window is given by

$$t_{ACRW}^{end} = t_{ACRW}^{start} + T_{maneuver}, \tag{56}$$

where $T_{maneuver} > 0$ is the desired duration of the maneuver. From this, the acceleration cost-gain is defined as

$$K_k^a := \begin{cases} k^a k_{maneuver}^a & \text{if } kh \in [t_{ACRW}^{start}, t_{ACRW}^{end}] \\ k^a & \text{otherwise} \end{cases} \tag{57}$$

where $k_{maneuver}^a \in (0, 1]$ is the cost reduction for acceleration usage within the ACRW. For the work presented here, we apply fixed values for T_{ample_time} and $T_{maneuver}$, however, a more qualified estimate of these parameters should be made for each vessel-to-vessel encounter based on factors such as the size, type, velocity and maneuvering capacity of the involved vessels. This is outside the scope of this paper, and is left for future work.

The start time for the PCRW is the same as for the ACRW

$$t_{PCRW}^{start} = t_{ACRW}^{start}, \tag{58}$$

and the end time is

$$t_{PCRW}^{end} = \max_{\mathcal{N}_{pri}}(t_{crit}^{exit}). \tag{59}$$

The PCRW extend from the time where the initial maneuver should start, until the trajectory is clear of the last vessel in $\mathcal{N}_{pri}$. The cost-gain for the tracking error is defined as

$$K_k^p := \begin{cases} k^p k_{maneuver}^p & \text{if } kh \in [t_{PCRW}^{start}, t_{PCRW}^{end}] \\ k^p & \text{otherwise,} \end{cases} \tag{60}$$

where $k_{maneuver}^p \in (0, 1]$ is the cost reduction for the position error within the PCRW. The PCRW reduces the cost of the tracking error from $\boldsymbol{x}_d$ when maneuvering, and hence also the motivation to converge back to $\boldsymbol{x}_d$ between TSs in the case of several TSs in $\mathcal{N}_{pri}$.

For each new iteration of the trajectory planner, the cost reduction profiles are time-shifted by the time since last iteration to match the new control horizon. Every time a new TS is included in $\mathcal{N}_{pri}$, it is assumed that a maneuver by the OS is needed, and new CRWs are calculated.

4.9 OCP formulation

Finally, the OCP can be defined on the form in (11), with the objective function given by (24), with gains according to (57) and (60). The equality constraints are on the form of (14), with the integrating function (13), where the $f(\boldsymbol{x}, \boldsymbol{v})$ is the system in (15), $\boldsymbol{x}$ is the system state and $\boldsymbol{a}$ is the control input. The set of inequality constraints is defined as

$$\boldsymbol{h} := \boldsymbol{h}_v \cup \boldsymbol{h}_a \cup \boldsymbol{h}_{TS} \cup \boldsymbol{h}_{stat} \tag{61}$$

where $\boldsymbol{h}_v$, $\boldsymbol{h}_a$, $\boldsymbol{h}_{TS}$ and $\boldsymbol{h}_{stat}$ are given by (29), (30), (44) and (50), respectively.

5 Simulations

In this section, simulation results are presented. First, an extensive set of vessel-to-vessel encounters in open waters are presented and discussed. These simulations cover a distributed subset of possible vessel-to-vessel

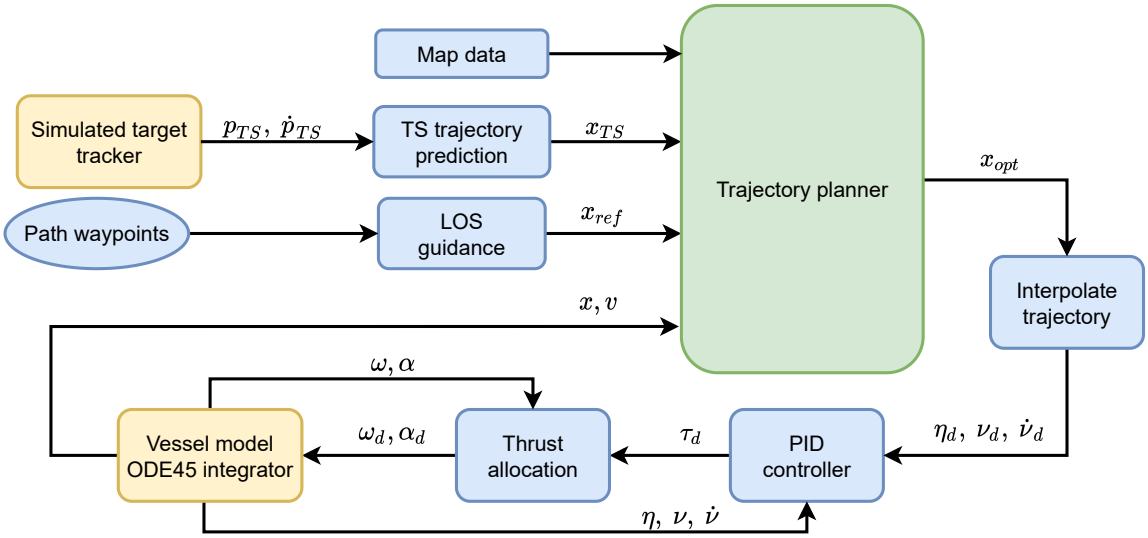

Figure 8: Guidance, navigation and control pipeline for the simulations. The internals of the green box are illustrated in Fig. 7.

encounters, and serve to demonstrate the completeness of the method in terms of COLREGs compliance with the rules from Section 3. Thereafter, we include a set of simulations from more complex urban environments where the presence of static obstacles and several maneuvering vessels demonstrate the capacity of the proposed method to handle an unstructured and highly relevant environment.

An overview of the simulator setup is shown in Fig. 8. The simulator is implemented in Matlab where the OS model is a 3DOF model of the milliAmpere experimental platform. The model parameters used in the simulations can be found in (Pedersen, 2019). In the simulations, the Matlab ODE45 solver is applied for state integration. The parameter values used in the simulations are given in tables 1 and 2.

The simulator consists of the following modules:

- The **Map data** module contains all static obstacles on the form of convex polygons.
- The **Simulated target tracker** module provides position and velocity states for all vessels that have a line of sight from the OS that is unobstructed by static obstacles.
- The **TS trajectory prediction** module makes a discretized trajectory prediction for the duration of the control horizon for each TS. The prediction is made based on a constant velocity model.
- The **Path waypoints** module is a set of waypoints that describes the desired transit route. Each waypoint has an associated reference speed.
- The **LOS guidance** module calculates $\boldsymbol{x}_{ref}$. This is done by simulating a kinematic vessel model starting at the initial conditions of the OCP, where the vessel tracks the path waypoints by means of a constant lookahead-distance LOS guidance method. The LOS guidance method inputs the path-waypoints and administers waypoint switching. The kinematic vessel model is simulated for the duration of the control horizon, where $\boldsymbol{x}_{ref}$ is constructed by discretizing the simulated trajectory with a timestep of h, and for N_p steps, resulting in a trajectory on the form of (20).
- The mid-level **Trajectory planner** module is the COLAV method described in Section 4. An overview of this module is shown in Fig. 7.
- The **Trajectory interpolation** module interpolates the discretized optimal trajectory $\boldsymbol{x}_{opt}$ to get reference signals for the PID controller.
- The **PID controller** module performs trajectory following by a velocity and acceleration feed forward PID controller.
- The **Thrust allocation** module realizes the generalized reference force $\boldsymbol{\tau}_d$ by calculating appropriate setpoints for the two azimuth thrusters.

5.1 Batch simulations

In this section, we present results for evaluating the completeness of the method in terms COLREGs compliance in vessel-to-vessel encounters without static ob-

Table 1: Rule-based parameters for the TS domain.

Parameter	SF	SO	OT_p	OTs	HO	GW	**Unit**
α_d	0	$\pi/4$	$\pi/3$	$\pi/3$	$2\pi/5$	$2\pi/5$	rad
α_{δ_s}	0	$\pi/2$	-$3\pi/4$	$3\pi/4$	$\pi/12$	-$\pi/8$	rad
c_{dyn}	10	10	40	40	60	60	s

Table 2: Non rule-based parameters.

Parameter	**Value**
N_p	150
h	4 s
k^p	$2.5 \times 10^{-5}\,\mathrm{m}^{-2}$
k^a	$50\,\mathrm{m}^2\mathrm{s}^{-4}$
$k^p_{maneuver}$	0.0005
$k^a_{maneuver}$	0.007
κ	0.7
δ_{dyn}	1 m
σ_{max}	4
σ_{min}	1
$T_{after\_pass\_padding}$	40 s
$T_{critical}$	140 s
$T_{crit\_stand-on}$	20 s
T_{ample_time}	120 s
$t_{maneuver}$	40 s
d_{σ_max}	20 m
d_{σ_min}	100 m
r_{free_max}	40 m
d_{crit}	50 m
k_l	0.50
N_{sect}	12
δ_{stat}	8 m

stacles. The results are produced through an extensive simulation study, with the OS and TS on straight line paths, where the TS keeps a constant course and speed in each simulation. The set of simulations is constructed by varying two parameters: the relative course χ_{rel} between the vessels, and the lateral offset, δ_{lat}, of the OS reference path from a point-of-collision at the origin of the local NED frame. The OS and TS waypoints are calculated so that both vessels will be at the origin after 200 s if $\delta_{lat} = 0$. The parameter χ_{rel} is iterated from 0 to 2π at steps of $\pi/16$, while the δ_{lat} is iterated from -200 m to 200 m at 10 m steps, resulting in a total of 1312 simulations. The OS and TS have a reference speed of 1.5 m/s and 1 m/s respectively. The OS path goes from west to east with $\chi = \pi/2$ while the TS path is adjusted for each χ_{rel}. A subset of the simulations are presented in figures 9 - 13 where all OS trajectories for a given TS course are combined in one figure.

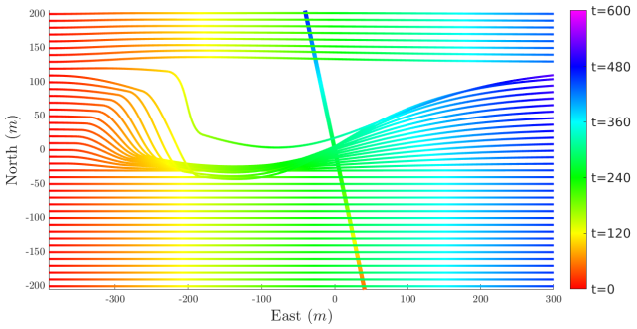

Figure 9: Batch 1: Give-way crossing.

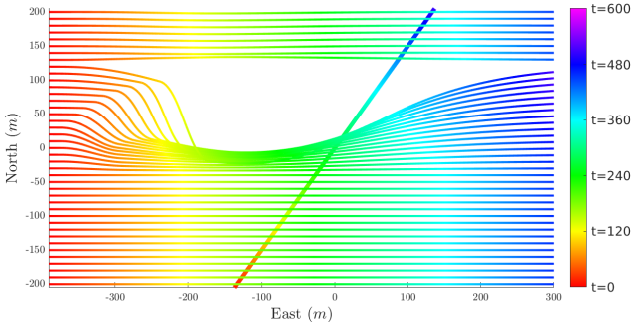

Figure 10: Batch 2: Give-way crossing.

Figures 9 and 10 show results from encounters where the OS has give-way obligations and is on a crossing course with the TS. One can see from the OS trajectories that the encounters are resolved by performing a starboard maneuver to pass behind the TS for a majority of the simulations where the OS has to maneuver from its reference trajectory to avoid TS domain violation. In one or two encounters in each of the figures, the OS instead performs a small port maneuver to pass in front of the TS. However, all encounters are resolved without domain violation, and in the situations where the OS maneuvers and still passes in front of the TS, it does so with such a margin that it does not impede the TS. The effects of the CRWs are also apparent from the OS trajectories between 50 s and 200 s into the transit, where the course change maneuver is visible and readily apparent, in compliance with Rule 8, in addition

to being made in ample time due to the ACRW and PCRW offset from the minimum t_{crit}^{enter}.

In Fig. 11, results from stand-on crossing encounters are presented. In these encounters, the TS is the give-way vessel and the OS has stand-on obligations, and shall keep its course and speed until it is apparent that the TS is not abiding its give-way duty, and the encounter can not be resolved by a maneuver from the TS alone. By only including stand-on vessels with a $tcpa^{+}_{critical}$ below a threshold value, this behaviour can be achieved, as demonstrated in Fig. 11. However, determining the threshold value $tcpa^{+}_{critical}$ is not trivial, where it should include considerations on several aspects of the TS, such as its maneuvering capabilities and vessel type. Such information can be acquired either through AIS or comprehended by the vessels situational awareness system based on exteroceptive sensors.

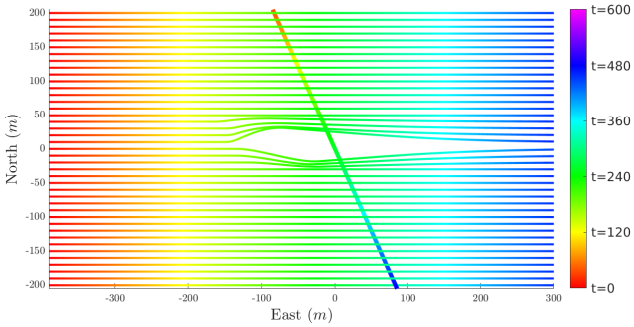

Figure 11: Batch 3: Stand-on crossing.

In Fig. 12, results from overtaking encounters are presented. From the figure, one can see that the OS gives way to the TS in all encounters. The effect of the CRWs is not as apparent in the overtaking encounters since the relative velocity between the vessels is small, and the duration of the manuever, and hence the reduced position cost window, extends throughout a majority of the control horizon. Additionally, the close to parallel courses of the OS and TS limits the need for course-change maneuvers from the OS to pass clear of the TS domain, and therefore the initial course change maneuver is less apparent than in the give-way crossing encounters. However, the maneuver is visible and made in ample time.

Finally, Fig. 13 shows results from head-on encounters. Also in these simulations, all encounters are resolved without violation of the TS domain. Similar to the give-way crossing encounters, the OS performs a readily apparent starboard maneuver in ample time, and passes the TS port to port in compliance with rules 8, 14 and 16.

Two substantial improvements are achieved by ap-

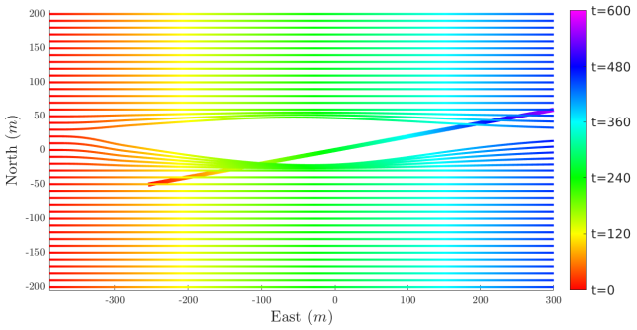

Figure 12: Batch 4: Overtaking.

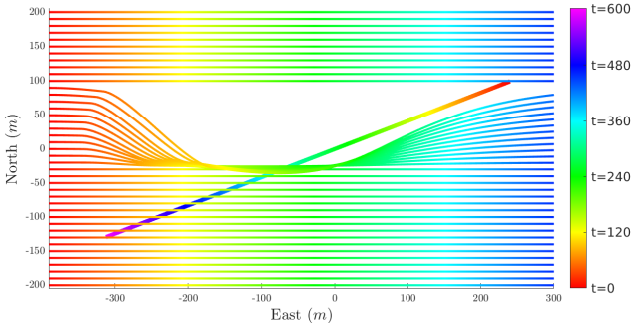

Figure 13: Batch 5: Head-on.

plying a deliberate trajectory planning approach, as opposed to the reactive method presented in (Thyri and Breivik, 2022a) which uses the same TS domain. Both improvements are clearly demonstrated in Fig. 14, where a batch of simulations for the deliberate and reactive method under similar conditions are presented. First, the reactive method has a stagnation problem that occurs when the OS is approaching the TS domain at a near right angle with no clear direction of deflection, as is apparent in the red frame in Fig. 14(b), where the OS trajectory slows down before deflecting to starboard. The trajectory planner that we propose in this paper avoids this problem as long as the control horizon extends beyond the duration of the encounter from the point at which the maneuver starts. The local optimal trajectory does not maneuver into these areas, as it results in both high acceleration and tracking error, and hence high cost. Furthermore, applying a deliberate planning approach, as opposed to the reactive one in Fig. 14(b), enables improvements w.r.t. the requirements of Rule 8, where "Any action taken to avoid collision shall, if the circumstances of the case admit, be positive, made in ample time and with due regard to the observance of good seamanship", which is achieved through the CRWs.

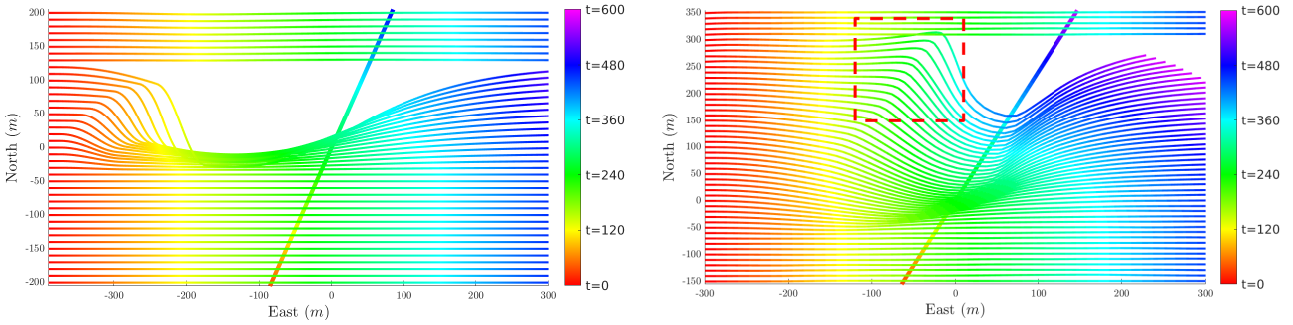

(a) Give-way crossing encounters with the trajectory planning method proposed in this paper.

(b) Give-way crossing encounters with the reactive COLAV method proposed in Thyri and Breivik (2022a).

Figure 14: Comparison of give-way encounters.

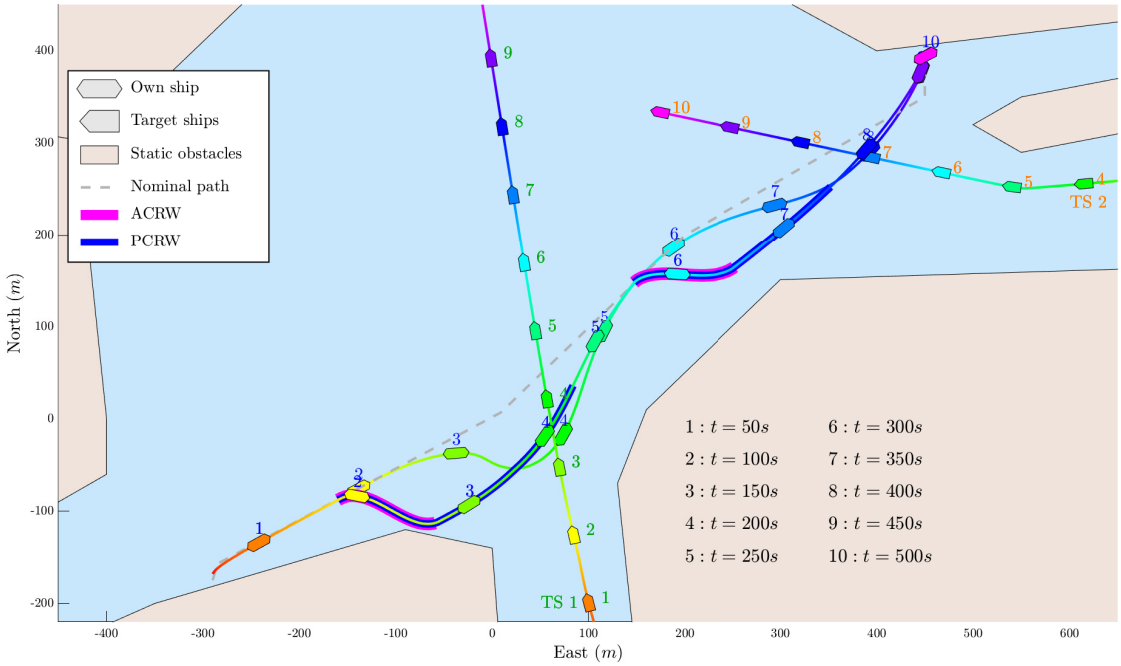

Figure 15: Simulation 1: Transit between two docking locations where the OS encounters two TSs in give-way encounters. The figure includes the OS trajectory for a run with and without CRWs. The TSs have identical behaviour in both runs.

5.2 Complex scenarios

In this section, we present a set of more complex simulations where the OS is maneuvering in a confined space with several other maneuvering vessels. These simulations demonstrates the proposed COLAV method's robustness in terms of COLREGs, where it handles a variety of encounters while adhering to the maneuvering principles of the rules presented in Section 3.1. An overview of each scenario is presented in a single figure with representations of the OS and each TS at matching 50 s intervals. The figures also show the OS nominal path and trajectory along with the trajectory of each TS. Furthermore, pink and blue lines are superimposed on the OS trajectory at the areas where the ACRWs and PCRWs are active and hence reduce the acceleration cost-gain and tracking error cost-gain respectively.

5.2.1 Simulation 1: Double give-way with and without CRWs

In this simulation, the OS performs a transit between two docking locations in an urban environment where

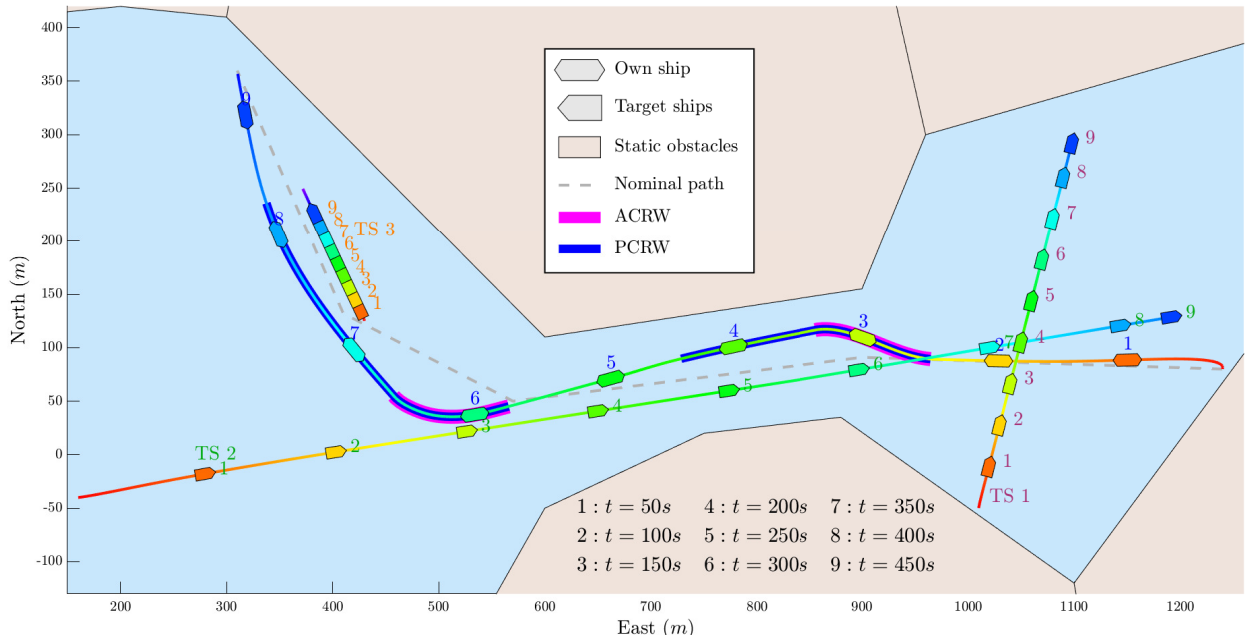

Figure 16: Simulation 2: Transit between two docking locations, with a stand-on, head-on and overtaking encounter.

it encounters two TSs in give-way crossing encounters. An overview of the simulation is given in Fig. 15, where the trajectory of the OS is included for a run both with and without the use of CRWs to calculate the tracking error and acceleration cost-gains.

From the overview in Fig. 15, one can see that the OS resolves both encounters in accordance with Rule 17 by performing a starboard maneuver and pass behind each TS in both runs. However, the effect of the CRWs are apparent, where for the run with CRWs, the avoidance maneuvers are of another magnitude, and come earlier compared to the run without CRWs.

This is further demonstrated in Fig. 17 where the OS course profile from the two simulations is shown. One can see that the CRWs motivate a maneuver that starts T_{ample_time} before the TCPA of each TS, where the course change maneuver is concentrated in a window of duration $T_{maneuver}$ to produce a positive and readily apparent course change maneuver. In the simulation with CRWs, the course change maneuvers have a magnitude of approximately 60°, where without CRWs, the first encounters is resolved by an initial gradual course change, followed by a sudden course change at close range, and the second encounter is resolved by a long-lasting continuous course change maneuver. This simulation clearly demonstrate the benefit of the proposed CRWs, where the maneuvering behaviour of the ownship can be made to comply with rules 8 and rule 16 by a small set of parameters.

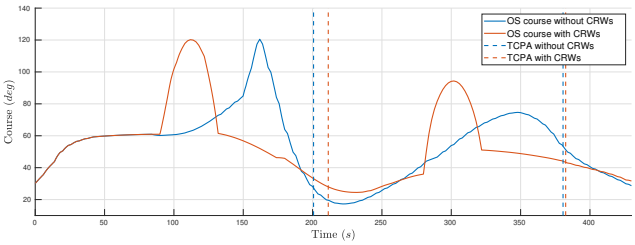

Figure 17: Simulation 1: Course profile for OS trajectory with and without CRWs.

5.2.2 Simulation 2: Stand-on, head-on and overtaking

In this simulation, the OS is transiting between two docking locations in an urban environment with three TSs. The first TS is met in a crossing encounter where the OS has stand-on obligations, the second TS is encountered head-on, and the final TS is met in an overtaking encounter where the TS is moving at a very low speed. An overview of the simulation is shown in Fig. 16. Due to the encounter type and the DCPA in the encounter with TS 1, the vessel is not included in $\mathcal{N}_{pri}$. This is apparent from Fig. 16 since no CRWs are assigned prior to the encounter. Hence, the OS keeps its stand-on obligations to TS 1 in accordance with Rule 17. As the encounter with TS 2 moves within the control horizon, TS 2 is included in $\mathcal{N}_{pri}$, and appropri-

Figure 18: Simulation 3: Transit between two docking locations, with a give-way crossing, stand-on crossing and a head-on/give-way encounter.

ate CRWs are assigned. As a result, the OS performs a course-change maneuver, and moves to its starboard side of the narrow area, to pass the oncoming vessel port to port. Note that at the CPA, the OS splits the available space between TS 2 and land close to equally between them, as $r_{free} < r_{free\_max}$. In the same way, when TS 3 is included in $\mathcal{N}_{pri}$, the CRWs are recalculated, resulting in a trajectory that continues straight when the nominal trajectory is turning, and performs the starboard maneuver at a later point. This prevents the OS from maneuvering onto a collision course with TS 3, and hence clearly demonstrate the OS's intention to give-way in the encounter in accordance with Rule 13. The OS completes the transit without collision while maneuvering in accordance with the COLREGs.

In this simulation, the OS transits between two docking locations in a harbour environment with traffic, where the TSs track reference trajectories that are maneuvering. An overview of the simulation is shown in Fig. 18. The OS is moving from east to west, while three other TSs are maneuvering within the area. The TSs are only visible to the planner when there is an unobstructed line of sight between the OS and the TS, and the predictions for the future TS trajectories assume constant velocity.

As the OS departs, it does not observe any other vessels. But, as it moves beyond the pier on its starboard side, it detects TS 1 exiting the northeast harbour and classifies the encounter as give-way crossing. Initially, the trajectory of the OS does not have a critical DCPA to the predicted trajectory of TS 1, but as TS 1 maneuvers, the estimated DCPA is reduced and TS 1 is included in $\mathcal{N}_{pri}$. This triggers the set of CRWs to be calculated. The CRWs are apparent from the pink and blue regions along the early parts of the OS trajectory. The resulting trajectory maneuvers to starboard to pass behind TS 1, in accordance with the Rule 15.

Later, the OS detects TS 2 exiting the harbour on its forward port side. This encounter is classified as a stand-on crossing. Despite TS 2 having a course that is on close to collision course with the OS, it does not have a t_{crit}^{enter} below the $T_{crit\_stand-on}$ threshold, and is therefore not included in $\mathcal{N}_{pri}$. As TS 2 subsequently maneuvers to starboard, the margins are increased, and it is therefore never included in $\mathcal{N}_{pri}$.

Lastly, the OS approaches TS 3 arriving from east.

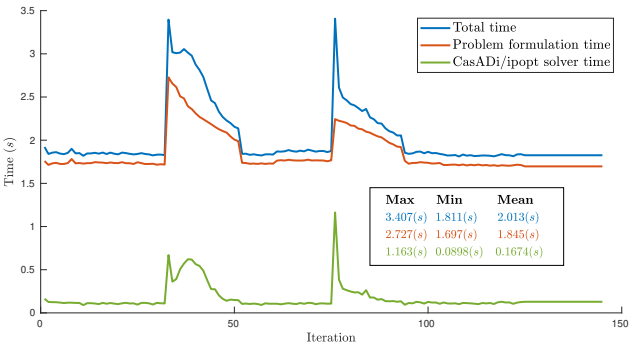

Figure 19: Runtime for the proposed algorithm for Simulation 3. The total time is split into the time for formulating the OCP, and the time the solver uses to find an optimal solution. The spikes clearly clearly indicate when TS 1 and TS 3 is included in $\mathcal{N}_{pri}$.

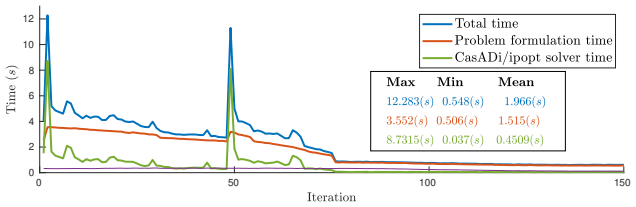

Figure 20: Runtime for the proposed algorithm for a very confined space simulation with 4 TSs that require avoidance maneuvers.

This TS is detected early, but due to its initial course, its predicted trajectory did not interfere sufficiently with the OS trajectory to be considered until it performed the starboard maneuver towards the harbour. It is then included in $\mathcal{N}_{pri}$, and a new set of CRWs are calculated. The OS performs a small starboard maneuver to pass TS 3 port to port, and eventually behind it. This OS maneuvers in accordance with both Rule 14 and Rule 15.

5.3 Runtime

For such a trajectory planning algorithm to be applied on a vessel, its runtime must support real-time operation. By this we mean that the period from a new input to an optimal trajectory is calculated should be of magnitude seconds or less to ensure that the optimal trajectory is still valid and relevant. When detecting a new TS that requires an avoidance maneuver, an updated trajectory should be calculated fast enough so that maneuvering in ample time is feasible. Additionally, a short runtime reduces jumps in tracking error when the initial part of the new trajectory deviates from the previous optimal trajectory, and hence dynamic feasibility and smooth transient behaviour is maintained. In Fig. 19, the runtime for the algorithm that we propose is displayed for Simulation 3, while Fig. 20 shows the runtime of a more complex scenario[2] with 4 TSs, where several of the vessels must be considered simultaneously.

Our code is written in Matlab with no particular regard to runtime, and runs on a Dell Precision 5540 with a 32 GB memory and an Intel Core i9-9880H processor running at 2.30 GHz. The results from Fig. 19 show that the algorithm uses on average 2 s, and a maximum of 3.407 s, on formulating and solving the OCP in Simulation 3. Furthermore, we see that the majority of the runtime comes from formulating, not solving, the OCP. This indicates some potential for further reduction in runtime by improving code efficiency. However, the runtime is within acceptable limits for real-time application. From Fig. 20, we see spikes in the runtime of about 12 s. The spikes come when TSs that require avoidance maneuvers are added to $\mathcal{N}_{pri}$, resulting in a large discrepancy between $\boldsymbol{x}_{initial\_guess}$ and $\boldsymbol{x}_{opt}$ combined with a large number of nonlinear constraints from the total set of vessels in $\mathcal{N}_{pri}$. The runtime analysis is not conclusive, however it indicates that the proposed algorithm is suitable for realtime operation in reasonably complex scenarios, while increasing traffic complexity can result in a runtime that extend beyond acceptable limits.

[2]The scenario is not included in the results of this paper, but an illustration of it can be viewed at: https://rb.gy/xxeruc

6 Conclusion and Future Work

An MPC-based approach to COLAV for ASVs that is compliant with COLREGs rules 8 and 13-17 has been presented. We propose to formulate and solve an optimal control problem for a simplified ASV model where the objective is to find a dynamically feasible trajectory that minimizes both the tracking error to some reference trajectory, and the induced acceleration. Collision avoidance with both static and dynamic obstacles is handled by assigning domains to each obstacle, and then formulating constraints for each domain.

Compliance with the encounter-type specific maneuvering requirements of rules 13-15 and 17 is handled by first classifying each vessel-to-vessel encounter, and then formulating constraints w.r.t. an encounter-type specific domain for each target ship (TS). The constraints are formulated so that if the trajectory does not violate them, the trajectory is in compliance with the relevant rule for that encounter.

Furthermore, compliance with rules 8 and 16 is facilitated through assignment of windows of reduced

cost on acceleration and tracking error, where the windows incentivize any avoidance maneuvers to fall within them. The position of the windows relative to an estimated time to a critical distance between the OS and TS is parameterized by a small set of intuitive parameters, and enables placement of the windows, and hence the maneuver, in ample time before close quarters.

The COLREGs compliance of the method is demonstrated through an extensive and systematic set of simulations of vessel-to-vessel encounters in open waters. The proposed method produces smooth maneuvers and resolves all encounters without collision, in accordance with the COLREGs rules 8 and 13-17.

Finally, we demonstrate the method in a relevant application through simulations of dock-to-dock transit in urban environments with several maneuvering vessels. The proposed method completes the transit in each case, and avoids collision or close quarters with the other vessels by performing COLREGs-compliant maneuvers. Lastly, the runtime of the method is demonstrated to be within feasible limits for real-time operation.

Future work includes:

- Improving compliance w.r.t. Rule 8 and Rule 16 by making an individual estimate of "ample time" for each vessel-to-vessel encounter.
- Further work on the encounter classification through improved intent inference.
- Full-scale experiments and closed-loop testing in combination with a target-tracking system based on exteroceptive sensors.
- Runtime improvements.

Acknowledgments

This work was supported by the NTNU Digital transformation project Autoferry and the Research Council of Norway through the Centers of Excellence funding scheme, project no. 223254.

References

Abdelaal, M., Fränzle, M., and Hahn, A. Nonlinear model predictive control for trajectory tracking and collision avoidance of underactuated vessels with disturbances. *Ocean Engineering*, 2018. 160:168–180. doi:10.1016/j.oceaneng.2018.04.026.

Abdelaal, M. and Hahn, A. NMPC-based trajectory tracking and collision avoidance of unmanned surface vessels with rule-based colregs confinement. In *Proc. IEEE Conference on Systems, Process and Control (ICSPC)*. pages 23–28, 2016. doi:10.1109/SPC.2016.7920697.

Cockcroft, A. N. and Lameijer, J. N. F. *Guide to the Collision Avoidance Rules*. Butterworth-Heinemann, 2012. doi:10.1016/C2010-0-68322-2.

Čorić, M. and Nikšić, M. Possibilities of Using Autonomous Green Vessels for Passenger Transport in Urban Environments. In M. Petrović, L. Novačko, D. Božić, and T. Rožić, editors, *The Science and Development of Transport—ZIRP 2021*, pages 91–109. Springer International Publishing, 2022. doi:10.1007/978-3-030-97528-9_7.

DB Schenker. DB Schenker plans to operate a zero-emission autonomous coastal container feeder for Ekornes ASA in Norway. 2022. URL https://www.dbschenker.com/global/about/press/autonomous-vessel-norway-788212. (Accessed: 6 May 2022).

Eriksen, B.-O. H. and Breivik, M. MPC-based mid-level collision avoidance for ASVs using nonlinear programming. In *Proc. 1st IEEE Conference on Control Technology and Applications (CCTA)*. Hawaii, USA, pages 766–772, 2017. doi:10.1109/CCTA.2017.8062554.

Eriksen, B.-O. H., Breivik, M., Wilthil, E. F., Flåten, A. L., and Brekke, E. F. The branching-course model predictive control algorithm for maritime collision avoidance. *Journal of Field Robotics*, 2019. 36:1222–1249. doi:10.1002/rob.21900.

Kuwata, Y., Wolf, M. T., Zarzhitsky, D., and Huntsberger, T. L. Safe maritime autonomous navigation with COLREGs, using velocity obstacles. *IEEE Journal of Oceanic Engineering*, 2014. 39(1):110–119. doi:10.1109/JOE.2013.2254214.

Lloyd's Register. ShipRight procedure - autonomous ships. *Cyber-enabled ships*, 2016.

Loe, Ø. A. G. *Collision Avoidance for Unmanned Surface Vehicles*. Master's thesis, Norwegian University of Science and Technology (NTNU), Trondheim, Norway, 2008. URL http://hdl.handle.net/11250/259696.

Martinsen, A. B., Bitar, G., Lekkas, A. M., and Gros, S. Optimization-based automatic docking and berthing of ASVs using exteroceptive sensors: Theory and experiments. *IEEE Access*, 2020. 8:204974–204986. doi:10.1109/ACCESS.2020.3037171.

Pedersen, A. A. *Optimization Based System Identification for the milliAmpere Ferry*. Master's thesis, Norwegian University of Science and Technology (NTNU), Trondheim, Norway, 2019. URL http://hdl.handle.net/11250/2625699.

Reddy, N. P., Zadeh, M. K., Thieme, C. A., Skjetne, R., Sørensen, A. J., Aanondsen, S. A., Breivik, M., and Eide, E. Zero-emission autonomous ferries for urban water transport: Cheaper, cleaner alternative to bridges and manned vessels. *IEEE Electrification Magazine*, 2019. 7(4):32–45. doi:10.1109/MELE.2019.2943954.

Ringbom, H. Regulating autonomous ships—concepts, challenges and precedents. *Ocean Development & International Law*, 2019. 50(2-3):141–169. doi:10.1080/00908320.2019.1582593.

RoBoat. Self-driving technology to transform urban waterways. 2021. URL https://roboat.org/. (Accessed: 14 December 2021).

Szlapczynski, R. and Szlapczynska, J. Review of ship safety domains: Models and applications. *Ocean Engineering*, 2017. 145:277–289. doi:10.1016/j.oceaneng.2017.09.020.

The Maritime Executive. China launches its first autonomous container ship service. 2022. URL https://www.maritime-executive.com/article/china-reports-first-autonomous-containership-entered-service. (Accessed: 6 May 2022).

Thyri, E. H., Basso, E. A., Breivik, M., Pettersen, K. Y., Skjetne, R., and Lekkas, A. M. Reactive collision avoidance for ASVs based on control barrier functions. In *Proc. 4th IEEE Conference on Control Technology and Applications (CCTA)*. Montreal, QC, Canada, pages 380–387, 2020a. doi:10.1109/CCTA41146.2020.9206340.

Thyri, E. H. and Breivik, M. A domain-based and reactive COLAV method with a partially COLREGs-compliant domain for ASVs operating in confined waters. *Field Robotics*, 2022a. 2:632–677. doi:10.55417/fr.2022022.

Thyri, E. H. and Breivik, M. Partly COLREGs-compliant collision avoidance for ASVs using encounter-specific velocity obstacles. In *Proc. 14th IFAC Conference on Control Applications in Marine Systems, Robotics, and Vehicles (CAMS)*. Copenhagen, Denmark, pages 1–7, 2022b.

Thyri, E. H., Breivik, M., and Lekkas, A. M. A path-velocity decomposition approach to collision avoidance for autonomous passenger ferries in confined waters. *IFAC-PapersOnLine*, 2020b. 53(2):14628–14635. doi:10.1016/j.ifacol.2020.12.1472. 21st IFAC World Congress.

Vagale, A., Bye, R. T., Oucheikh, R., Osen, O. L., and Fossen, T. I. Path planning and collision avoidance for autonomous surface vehicles II: A comparative study of algorithms. *Journal of Marine Science and Technology*, 2021a. 26:1307–1323. doi:10.1007/s00773-020-00790-x.

Vagale, A., Oucheikh, R., Bye, R., Osen, O., and Fossen, T. I. Path planning and collision avoidance for autonomous surface vehicles I: A review. *Journal of Marine Science and Technology*, 2021b. 26:1292–1306. doi:10.1007/s00773-020-00787-6.

Wärtsilä. Wärtsilä to develop autonomous, zero emission barge for port of Rotterdam. 2021. URL https://www.wartsila.com/media/news/27-05-2021-wartsila-to-develop-autonomous-zero-emission-barge-for-port-of-rotterdam-2921606. (Accessed: 4 November 2021).

Xue, Y., Wang, X., Liu, Y., and Xue, G. Real-time nonlinear model predictive control of unmanned surface vehicles for trajectory tracking and collision avoidance. In *Proc. 7th International Conference on Mechatronics and Robotics Engineering (ICMRE)*. Budapest, Hungary, pages 150–155, 2021. doi:10.1109/ICMRE51691.2021.9384818.

Zeabuz. Zero emission autonomous urban mobility. 2022. URL https://zeabuz.com. (Accessed: 25 January 2022).

Öztürk, Ü., Akdağ, M., and Ayabakan, T. A review of path planning algorithms in maritime autonomous surface ships: Navigation safety perspective. *Ocean Engineering*, 2022. 251:1–19. doi:10.1016/j.oceaneng.2022.111010.